Chapter Seven: The Second Cloud and Aerosol Characterisation Experiment (CLACE 2)

7.1 Introduction

Supersaturations of several hundred percent are required for the homogeneous formation of water droplets in particle free air [*Pruppacher and Klett, 1980; Seinfeld and Pandis, 1998*]. This does not occur in the atmosphere because of the sufficient concentrations of aerosol particles that act as cloud condensation nuclei (CCN) at supersaturations that are well below 2%. The ability of a given particle to serve as a CCN depends on its size, chemical composition as well as the supersaturation [*Seinfeld and Pandis, 1998*]. For example, if the ambient relative humidity (RH) does not exceed 100%, no particles will be activated and cloud cannot be formed. The relative humidity (RH) of an air parcel increases as it is lifted vertically in the atmosphere. At the deliquescence point, the water-soluble components of the CCN dissolve. The CCN grows by the addition of water with the continuing increase in RH. If a CCN reaches its critical diameter, (which depends on the particle chemical composition and dry size [*Seinfeld and Pandis, 1998*]) it will continue to grow as long as the air parcel remains above its equilibrium supersaturation. Particles that do not reach their critical diameter are not activated, though may be increased in size by the addition of water. Cloud optical properties are controlled by the sizes and numbers of the droplets in the cloud, which are, in turn, governed by the availability of atmospheric particles that serve as CCN. *Twomey* [*1974; 1977*] suggested that an increase in atmospheric aerosols from anthropogenic emissions would lead to smaller cloud droplets because the same amount of cloud liquid water content is distributed among more condensation nuclei. For the same liquid water content, a cloud with more numerous, but smaller, drops has a higher albedo than one with fewer, larger, drops. This phenomenon is known as the first indirect climatic effect of aerosols, which despite being widely discussed in the scientific community remains poorly understood and quantified [*IPCC, 2001*].

Understanding the properties of clouds is currently limited by difficulties at the fundamental level of adequately describing the processes of cloud droplet activation and growth. Models of cloud formation [*Shulman et al., 1996*] based on laboratory studies with idealised composition of nuclei suggest that organic solutes significantly lower

surface tension; one of the parameters determining cloud droplet population. *Facchini et al.,* [*1999*] reported measurements on samples of cloud water from the Po Valley, Italy, that showed a large decrease in surface tension, by up to one-third relative to pure water, for realistic concentrations of organic solutes expected to exist in growing droplets. If such large surface tension changes occur in cloud droplets near the critical size for nucleation, they may lead to an increase in the droplet population and hence in cloud albedo. The error produced in ignoring this effect has been estimated to be comparable to other calculated direct and indirect influences of aerosols on scattering and absorption of solar radiation [*Facchini et al., 1999b*]. More data on the composition and properties of the organic material in the atmosphere are needed in order to better understand their role in the cloud formation process, and enable model studies to better quantify the direct and indirect radiative forcing effects of aerosols.

Various groups have investigated aerosol activation processes using several experimental approaches to compare the properties of cloud droplets with aerosol particles. For example, the properties of cloud droplets with pre-cloud aerosols were compared in polluted and clean environments [*Choularton, 1995; Choularton et al., 1997; Bower et al., 1999; Bower et al., 2000a; Bower et al., 2000b; Flynn et al., 2000*], interstitial aerosols (i.e. particles that do not activate into cloud droplets) have been compared with pre-cloud aerosols [*Svenningsson et al., 1997; Martinsson et al., 1999*] and cloud droplets were compared with the in-cloud interstitial aerosols [*Schwarzenboeck et al., 2000*]. Airborne studies in- and below-cloud were conducted [*Gillani et al., 1995; Leaitch et al., 1996*]. *Henning et al.*, [*2002*] have investigated the size-dependent aerosol activation at the Jungfraujoch high-alpine research station (Figure 7.1) by measuring the interstitial and total aerosols (i.e. the sum of particles that were activated or scavenged plus those that remained interstitial) with the same experimental setup alternating every 6 min, providing a quasi-parallel measurement of the total and interstitial aerosol without assuming information on the air parcel trajectory as is case for most of the other approaches mentioned above. However, these studies only reported very limited information on the aerosol chemical composition, in particular its organic fraction.

The second Cloud and Aerosol Characterisation Experiment (CLACE2) was carried out jointly by UMIST and the Paul Scherrer Institute (PSI), Switzerland, from 28/06 to 17/07/02 at the Jungfraujoch high-alpine research station (3580 m asl). The experiment aimed to couple the highly time and sized resolved chemical composition information from the AMS to a suite of other aerosol and microphysical instruments in a variety of air masses in the lower free troposphere at the Jungfraujoch in order to investigate the interaction between cloud and aerosols using the same sampling methodology introduced by *Henning et al.*, [*2002*]. Results from this collaboration are presented and discussed in this chapter. In the first part of the chapter, the variability of the aerosol chemical composition and size distribution at the Jungfraujoch during CLACE2 is discussed in relation to local weather conditions and history of the air masses arriving at the site. The second part attempts to characterise the cloud-aerosol interaction in various types of air masses and conditions by linking these observations to the subsequent microphysical properties of the cloud using a series of case studies.

Figure 7.1: A picture of the sphinx laboratory at the Jungfraujoch high-alpine research station (3580 m asl), Switzerland.

7.2 Experimental methodology

7.2.1 Site description

The experiment was carried out from the Sphinx Laboratory located at the Jungfraujoch high-alpine research station (46.33 ^{o}N, 7.59 ^{o}E, 3580 m asl). The station is located on the northern side of the main central European Alpine chain in the Jungfraujoch region, Switzerland (Figure 7.2). It is surrounded by glaciers and rocks, and no local vegetation is present. The Jungfraujoch boasts the highest European railway station and is easily accessible throughout the year. Local emissions from the station and the tourist facilities

are negligible since all heating is electrical [*Baltensperger et al., 1997a; Baltensperger et al., 1998*]. The observation of cloud and aerosol parameters at the Jungfraujoch have been conducted by the Paul Scherrer Institute and others since 1988 and have established the site as suitable to investigate the chemistry and physics of the free troposphere above a continental region [*Baltensperger et al., 1997a*]. The research station is part of the Swiss National Monitoring Network for Air Pollution (NABEL), the Swiss Meteorological Institute (SMI) as well as the Global Atmospheric Watch (GAW) programme of the World Meteorological Organisation (WMO).

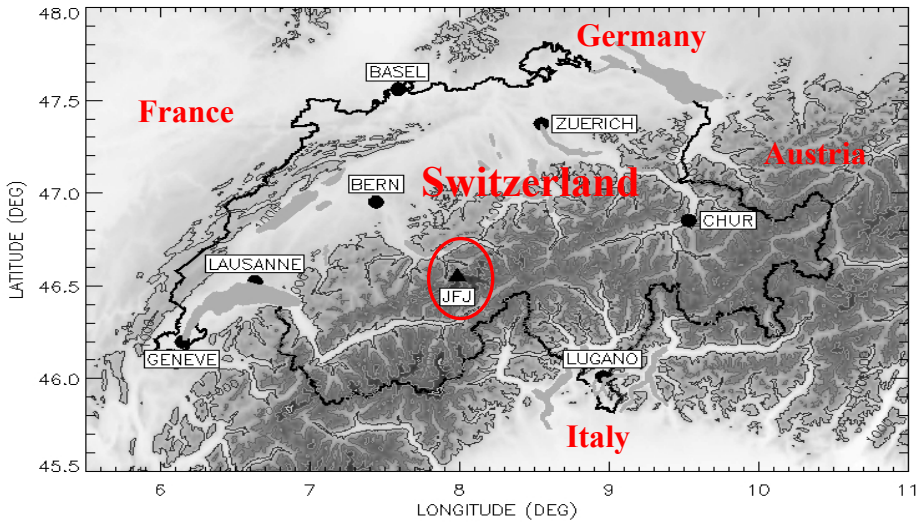

Figure 7.2: a map illustrating the location of the Jungfraujoch (JFJ) research station.

7.2.2 Sampling methodology

During cloudy conditions, initial separation of cloud droplets and the aerosol was performed using different inlet systems, Figure 7.3. It is important to note the cloud droplets were all liquid since the summertime temperature at the Jungfraujoch was mostly between –8 and 5 ^{o}C. A heated inlet (25 ^{o}C), designed to evaporate all cloud droplets at an early stage of the sampling process was used to collect the *total aerosol* population, including the non-activated fraction, to the suite of measuring instruments. A second inlet was used to remove cloud droplets using an impactor with a 1 µm upper size cut operating at ambient temperature (i.e. without heating). The particles sampled are either un-activated or have not yet grown to sizes greater than 1 µm and are known as *interstitial aerosol* particles. By duplicating measurements on the total and interstitial aerosol samples, cloud droplet properties can be derived by differencing. During cloud

free periods both inlets sample similar aerosol particles. These inlets were successfully validated during the first CLACE experiments [*Weingartner et al., 1999; Henning et al., 2002*].

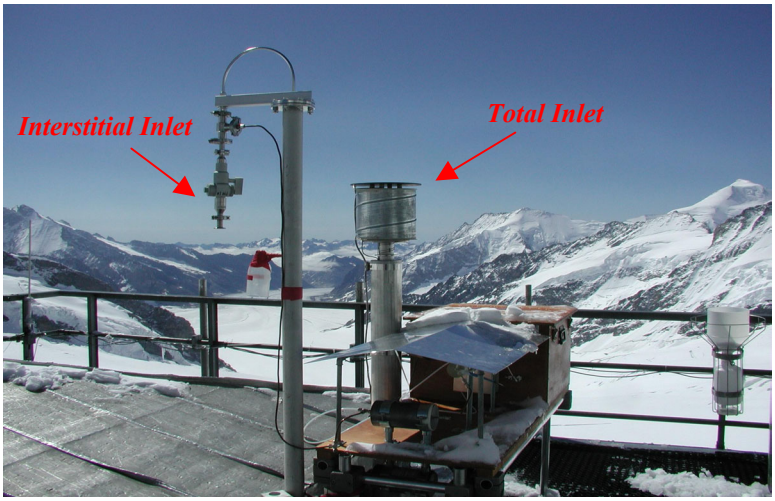

Figure 7.3: A picture of the inlets used to sample total and interstitial aerosol particles at the Jungfraujoch during CLACE2.

Ambient air was continuously sampled into the laboratory through both *total* and *interstitial* inlets and switching valves were used to alternate between the pair of them every 6 min, to feed the main sample manifold delivering ambient air to the AMS, a CPC and a scanning mobility particle sizer (SMPS). As most of the aerosol instruments sampled through the same line the sampling time of 6 min was used in order to match the minimum time required to perform a full scan by the slowest instrument. In this case this was the SMPS, which was operated by PSI during the experiment. The AMS logging software was modified to save automatically upon receiving an external signal from a TTL switch on connected to the inlet power switch delivering 0 and 5 volts for the interstitial and total inlets, respectively. On a change in the digital signal the AMS logging software was configured to save two files containing the mass spectral and size distribution data, and wait for a predefined 18 s period for the line to be purged before restarting the measurement cycle and averaging the new data again. The switching inlet was used from 18:30 on 4th July to the end of the experiment. Prior to this, AMS data were collected through the total inlet with 15 min averaging time.

7.2.3 Instrumentation

Results in this chapter are based on measurements of aerosol size distribution and chemical composition provided by the AMS. In addition, a condensation particle counter (TSI, model 3025a) was used to measure the aerosol number concentration. The aerosol hygroscopic properties were measured using a Hygroscopic Tandem Differential Mobility Analyser (HTDMA) system [*Weingartner et al., 2002*], which was operated at ambient temperature by the Paul Scherrer Institute. A forward scattering spectrometer probe (FSSP) was used to measure the cloud droplet size distribution, number concentration and derive the liquid water content. This instrument, developed by Droplet Measurement Technologies (DMT), is an upgraded version of the standard Particle Measuring Systems (PMS) *FSSP-100*, originally described by *Knollenberg* [*1981*] and has found widespread use in the cloud physics community. Its operation and characteristics have been discussed extensively in the literature [*Baumgardner et al., 1985*]. During CLACE-2 experiment the FSSP was operated on size range 1 ($2.0 < D_p <$ 47.0 μm) with 20 separate size bins. Local meteorological data (e.g. wind speed and direction, temperature, humidity, pressure, radiation) were available from the automatic meteorological station of the Swiss weather service located in the Sphinx observatory.

7.3 Variability of aerosol chemical composition and size distribution at the Jungfraujoch

7.3.1 Overview of aerosol mass concentration and size distribution

Time series of the mass concentrations (μg m^{-3}) of the non-refractory nitrate, sulphate, ammonium and organic components sampled through the total inlet throughout the duration of CLACE2 are shown in Figure 7.4. Averaged mass concentrations of each of the four major chemical components along with their concentration ranges and averaged fractional contributions to total measured mass are summarised in Table 7.1. The negative values of the minimum concentrations are caused by noise in the signal at the associated mass fragments. Even though the averaged mass concentrations are 1.22 μg m^{-3} for organics and 0.5 μg m^{-3} or less for inorganic species, the mass concentrations of most species were frequently higher, exceeding 3 μg m^{-3} and 1 μg m^{-3} for organic and individual inorganic species, respectively.

A mass spectrum averaged over the entire sampling duration and normalised to the peak of highest intensity is shown in Figure 7.5. Results illustrate that the aerosol chemical composition at the Jungfraujoch during CLACE2 was mostly dominated by organic material and to a lesser extent by sulphate and ammonium, with an occasional increase in nitrate concentration. On average, organic material composed 54% of the total measured aerosol mass, while the three inorganic components accounted altogether for 46% of the measured mass. These results are in close agreement with previously reported values of the inorganic and organic aerosol composition at the Jungfraujoch using off-line analysis methods [*Krivacsy et al., 2001a*]. A second study demonstrated the predominance of the ammonium sulphate component of the inorganic ionic composition of aerosol particles at the Jungfraujoch during summer time [*Nyeki et al., 1996b*]. It has been reported that ammonium, sulphate and nitrate account for 96% of the composition of inorganic ions at the Jungfraujoch [*Krivacsy et al., 2001a*].

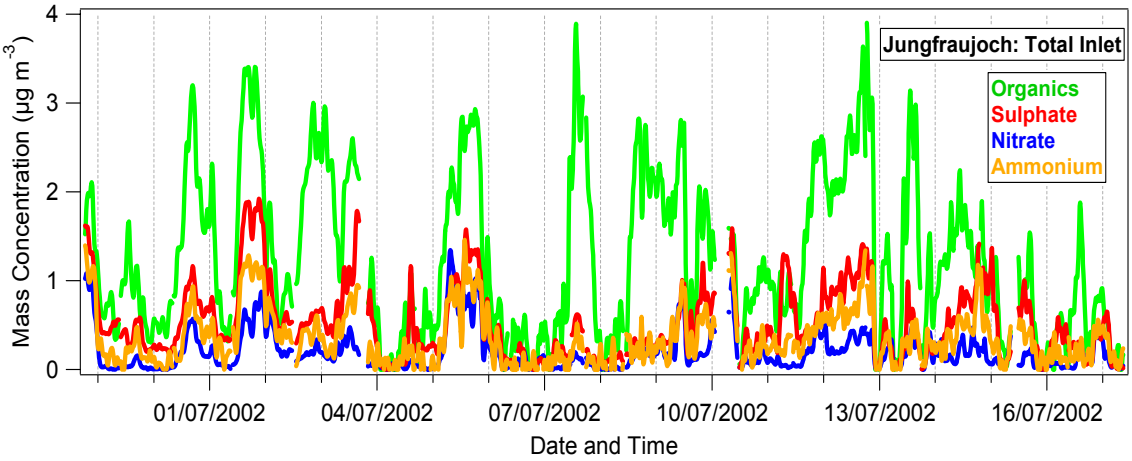

Figure 7.4: Mass concentration time series of the aerosol chemical components sampled using the total inlet during CLACE 2. The ticks of the X-axis correspond to midnight of each day.

Species	Average Concentration (μgm^{-3})	(min – max) (μgm^{-3})	Fractional Contribution (%)
Organics	1.22	(-0.23 – 3.90)	54
Sulphate	0.50	(-0.02 – 1.92)	22
Ammonium	0.33	(-0.24 – 1.46)	15
Nitrate	0.20	(-0.02 – 1.34)	9
Total	2.26	(-0.20 – 7.21)	-

Table 7.1: Summary of the average, minimum and maximum mass concentrations and the fractional contributions to total mass of the aerosol chemical components sampled through the total inlet at the Jungfraujoch during CLACE2.

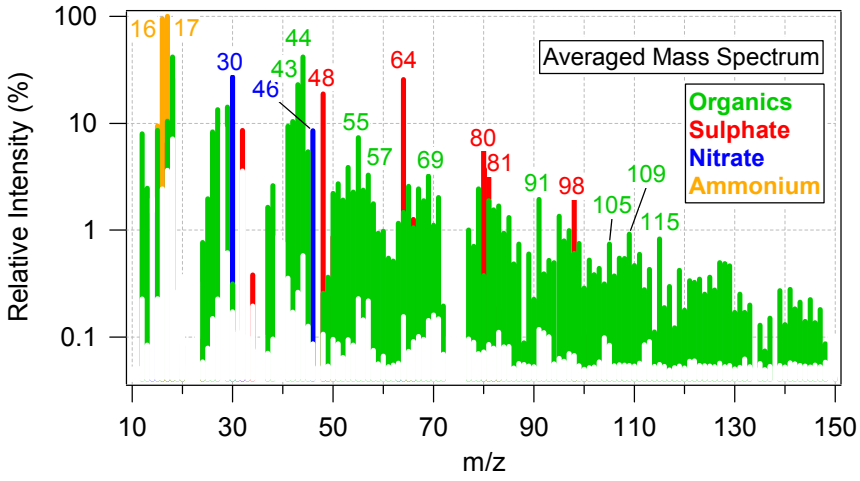

Figure 7.5: A mass spectrum averaged over the entire duration of CLACE2.

The time series of the aerosol chemical components (Figure 7.4) show a clear increase in the mass concentration, frequently starting after midday. Though this is most notable for organics, the inorganic components also display the same variability. In order to investigate whether the data follow a diurnal trend, average diurnal patterns for the entire data set were calculated from the time series of the organics, sulphate, ammonium, and nitrate mass concentrations. Figure 7.6 presents these diurnal data in the form of boxplots, showing the median and 5, 25, 75 and 95% percentiles for each component as well as the means of the mass concentrations for every hour of the day. The results as shown in Figure 7.6 show diurnal patterns in all four components with the mean values exhibiting a maximum during the afternoon and evening hours (approximately 13:00 - 22:00), and a minimum during the early hours (approximately 00:00 - 07:00). This pattern is most noticeable for organics, sulphate and ammonium and to a lesser extent for nitrate. This may be explained by the relative low mass concentrations of nitrate. Previous studies at the Jungfraujoch have determined that an annual cycle of aerosol concentration exists, exhibiting a maximum in July-August and a minimum in January-February, with a pronounced diurnal cycle of aerosol concentration mostly during the spring/summer period [*Baltensperger et al., 1991; Nyeki et al., 1996a; Baltensperger et al., 1997a; Baltensperger et al., 1997b; Lugauer et al., 1998; Weingartner et al., 1999*].

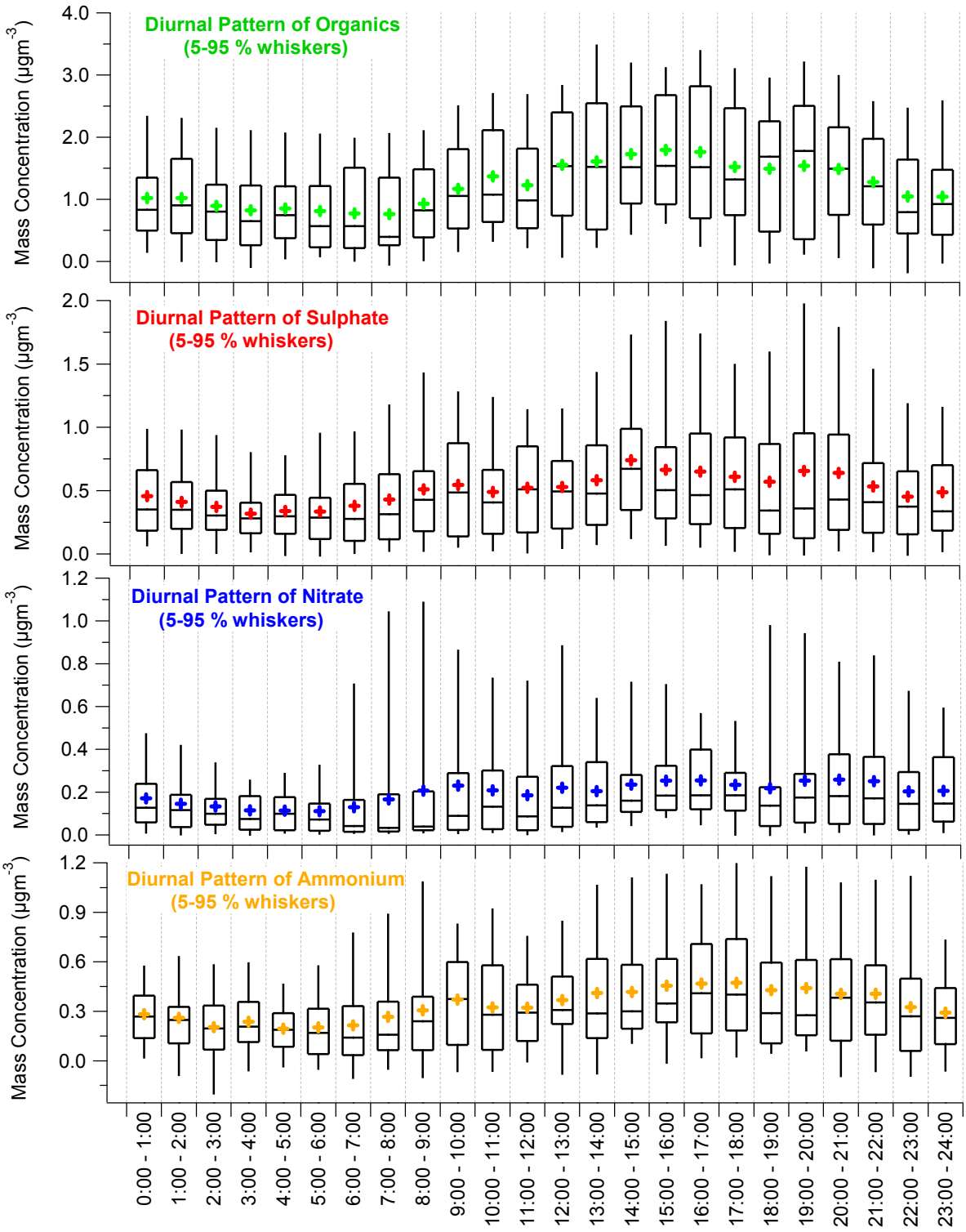

Figure 7.6: Diurnal patterns of the total measured aerosol chemical components at the Jungfraujoch during CLACE2.

In those studies, the diurnal cycle has been found to be influenced by the free troposphere from about 01:00 – 11:00 and influenced by the planetary boundary layer (PBL) from about 11:00-01:00. The relatively high aerosol concentrations were explained by vertical transport associated with the growth of the convective boundary layer during summertime rather than increased aerosol formation by homogenous and heterogeneous nucleation [*Baltensperger et al., 1997a*]. Vertical transport was found to be the process governing the aerosol concentration while the influence of horizontal transport was only of second order [*Baltensperger et al., 1997b*].

Mass size distributions of organics, sulphate, nitrate, and ammonium averaged over the entire sampling duration are shown in Figure 7.7. Although the distributions are averaged over the duration of the entire experiment, they do provide an overall picture of the modal behaviour of the aerosol chemical components during CLACE2. The data show that all four components have a single distinct mode with a peak between 300 - 400 nm. In addition, the organic mass size distribution appears to be broader, compared to the inorganic species, with a shoulder at about 200 nm. The observed distributions indicate that particles of different sizes were occasionally measured at the Jungfraujoch, where the dominance of the organic fraction increased with decreasing particle size. This behaviour is similar to that shown in the chapter 5 in rural areas such as Langley. However for much of the time the organic mode was similar to the inorganic mass size distributions, indicating that the aerosol may be chemically internally mixed.

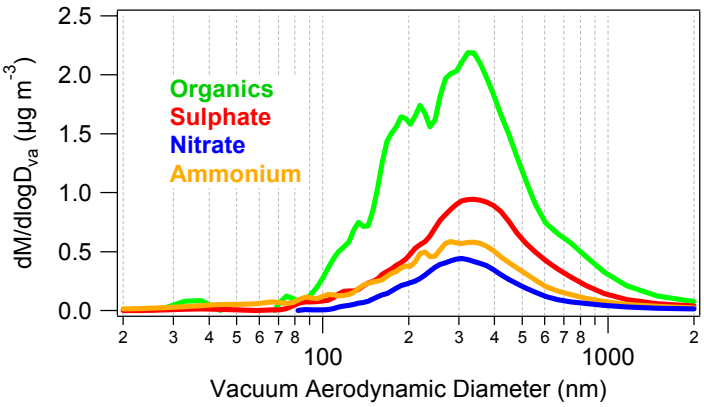

Figure 7.7: Mass size distributions of the aerosol chemical components averaged over the entire CLACE2 duration.

Time series of the mass size distributions of the four major aerosol chemical components are presented in Figure 7.8. The highly time-resolved data confirms the presence of a consistent sulphate and nitrate mass mode around 300 – 400 nm at the Jungfraujoch at all times when the particle mass concentration is above the detection limit. On the other hand, it is more difficult to see the modal distributions of the

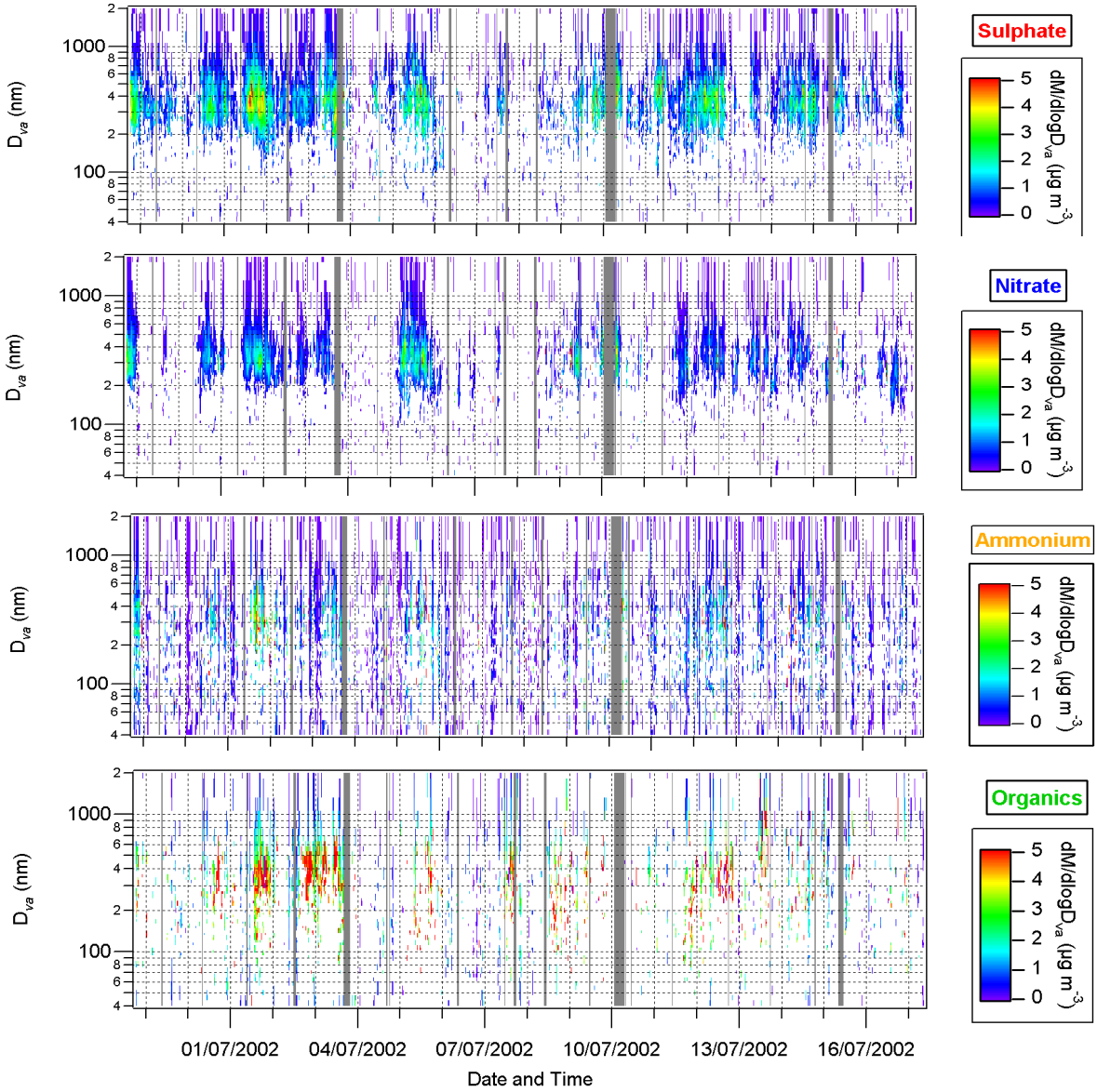

Figure 7.8: Time series of the mass size distributions of the total aerosol chemical components during CLACE2.

ammonium and organic components due to the low signal to noise associated with their mass fragments at high sampling time resolution. It is clear from Figures 7.7 and 7.8 that the distinct small organic mode observed in urban locations (see chapter 5, sections

5.3 and 5.4) is no longer present at the Jungfraujoch. As discussed in chapter 5 (sections 5.3 and 5.5), this is typical of aerosol distributions measured at locations away from source points and indicates that the particles measured at the Jungfraujoch were aged after being transported from other regions.

7.3.2 Characteristics of the aerosol organic fraction at the Jungfraujoch

The mass spectral signature of the aerosol organic fraction at the Jungfraujoch has been discussed in the chapter 5 (sections 5.5 and 5.6.3). Mass fragments 44 and 43 dominate the mass spectrum, indicating that the organic fraction is mainly composed of highly oxygenated compounds of secondary nature, such as carbonyls and dicarboxylic and poly acids. Results in section 5.6.3 showed that mass fragment 44, the AMS signature of oxidised organic compounds and humic-like substances, accounts, on average, for about 14% of the total organic mass at the Jungfraujoch. Mass size distributions of the key organic mass fragments *m/z* 44, 43 and 57 measured at the Jungfraujoch have also been presented in section 5.5 (see Figure 5.9), where the modal behaviours of those three key organic masses at various urban and non-urban locations were discussed. The dominance of mass fragments 44 and 43 in the accumulation mode and the lack of significant contributions of mass fragments 57 and 43 in the small mode indicated that the aerosol organic fraction at the Jungfraujoch is largely composed of highly oxidised compounds and that secondary organic aerosols are more significant than primary compounds during the sampling period. These results are supported by a previous report of oxygen-to-carbon atomic ratio of 0.55 at the Jungfraujoch, which implies that the organic compounds are highly oxygenated at this location [*Krivacsy et al., 2001a*].

These conclusions are emphasised in Figure 7.9, where the mass concentrations of the three mass fragments discussed above are scatter plotted against the total organic concentration for the entire sampling period. The slopes and Pearson's *r* values of the correlation of each mass fragment with the total organic mass are summarised in the figure. Results show that *m/z* 44 followed by *m/z* 43 have the highest slope and Pearson' r values, while mass concentration of *m/z* 57 does not appear to increase with increasing total organic mass.

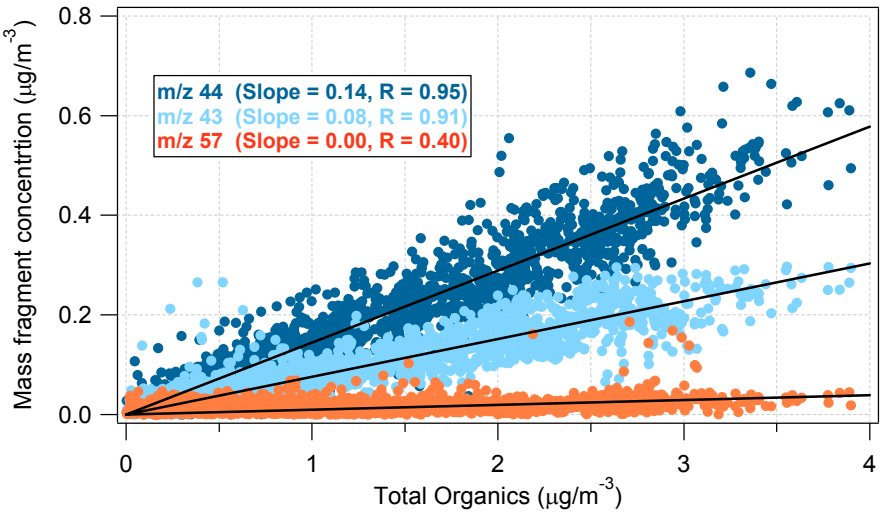

Figure 7.9: A scatter plot of the mass concentration of the organic mass fragments 43, 44 and 57 versus the total organic mass concentration for the entire CLACE2 dataset.

7.3.3 Classification of data according to local weather conditions

7.3.3.1 Comparison of the size distribution and mass concentration of aerosol chemical components at the Jungfraujoch during clear and cloudy conditions

The Jungfraujoch experiences a high frequency of clouds throughout the year. It has been reported that clouds are present at the site for 37% of the time as an annual average [*Baltensperger et al., 1998*]. To compare the size-resolved chemical composition of the aerosol particles at the Jungfraujoch during in- and out- of cloud events, the *total inlet* data for each chemical component were averaged accordingly and are shown in Figure 7.10, along with the averaged distributions during all conditions over the entire sampling duration. Cloud droplet number concentrations measured using the FSSP, were used to classify the dataset into clear sky and cloudy conditions using a threshold concentration of 10 droplets/cm^3. Results show that the modal behaviors and shapes of the mass size distributions of the individual aerosol chemical components do not appear to vary between in- and out- of cloud conditions. On the other hand, the mass concentrations of the inorganic components (sulphate, nitrate, ammonium) appear to be enhanced during cloudy periods. This is most pronounced for ammonium and nitrate, while it does not appear to be the case for the organic fraction of the particles, where little difference has been observed between the two cases. These results imply that

significant fraction of the inorganic mass observed at the Jungfraujoch is associated with cloud events, while the organic mass concentration appear to be similar during in and out of cloud events.

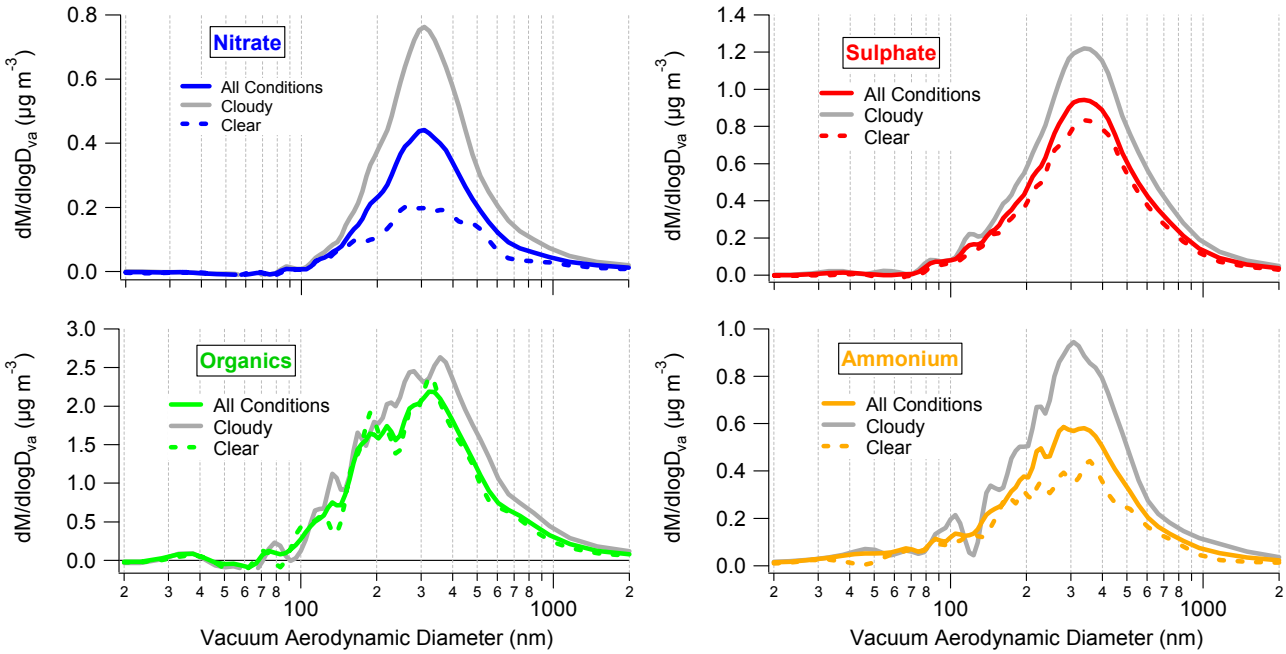

Figure 7.10: Mass size distributions of the aerosol chemical components averaged over all cloudy and clear periods in addition to all conditions during CLACE2.

To further illustrate these findings, time series of the mass concentrations of the aerosol chemical components are shown in Figure 7.11, where clear and cloudy periods are identified using the background blue and gray colours, respectively. The white gaps are periods where FSSP data were not available. A close inspection of the data in Figure 7.11 reveal that enhanced organic mass concentrations were observed during cloudy as well as clear conditions, while enhanced mass concentrations of inorganic components were mostly associated with cloud events. These results and the observed mass concentration diurnal trends (section 7.3.1) suggest that most of the clouds observed at the Jungfraujoch during CLACE2 were formed by lifting of air masses rather than by regional high level advection.

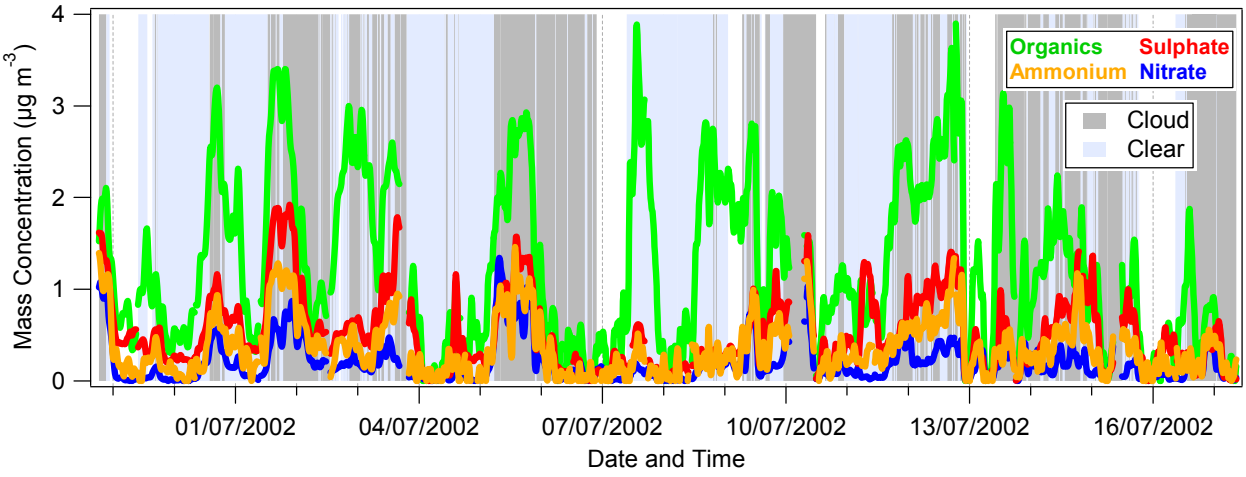

Figure 7.11: Identification of the cloudy and clear periods during CLACE2 and the corresponding chemical composition of total aerosol.

7.3.3.2 Effect of local wind direction and speed on the size distribution and mass loading of aerosol chemical components at the Jungfraujoch

The location of the Jungfraujoch, between the Jungfrau (4158 m) and Monch (4089 m) mountains, channels the local horizontal wind flow in either a north-western (NW) or south-eastern (SE) direction. In the north-westerly wind direction, air from the Swiss plateau is advected to the Jungfraujoch, while during south-easterly directions, the air comes from the inner Alpine area. The data shown in Figure 7.12 illustrate that relatively high levels of pollution were associated with the SE local wind direction, where particle number concentrations up to 4000 cm^{-3} were observed, whereas cleaner conditions with particle number concentrations mostly below 1000 cm^{-3} were associated the NW direction. Figure 7.12 shows the averaged mass size distributions of the sulphate, nitrate, ammonium and organic components of the aerosol observed during periods of either SE or NW local wind direction and wind speed higher than 2 m s^{-1}. The data show little differences in the modal behaviour and shape of the mass size distributions of the four chemical components in the SE and NW directions. However, the mass concentrations of all components are shown to be substantially higher during periods of SE local wind direction.

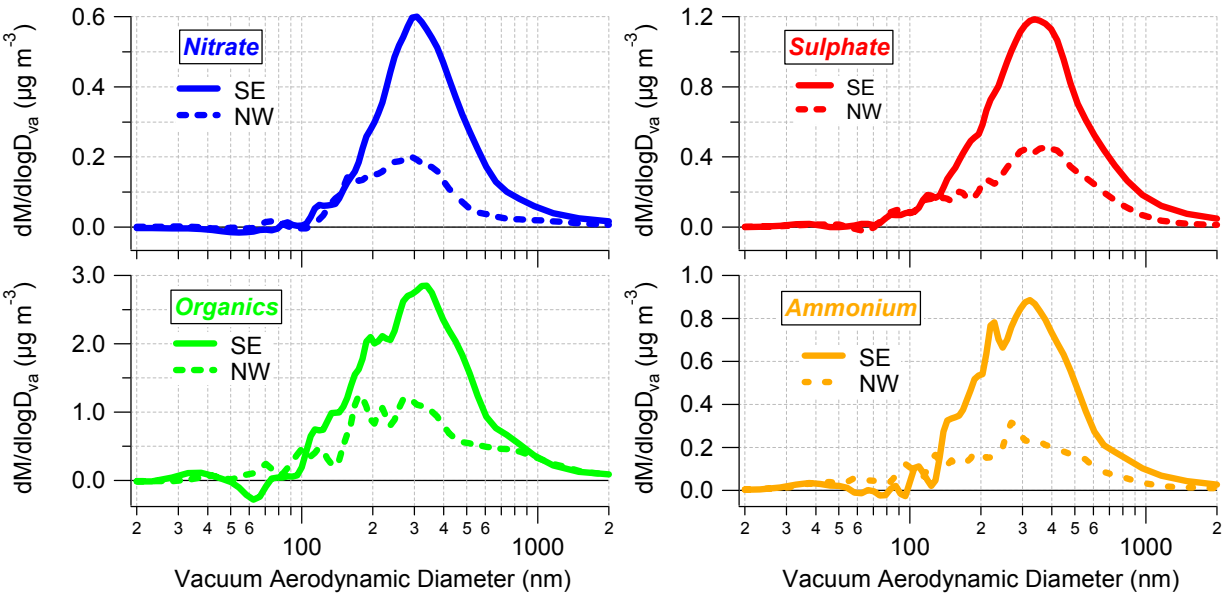

Figure 7.12: Averaged mass size distributions of the aerosol components sampled through the total inlet and separated according to local wind direction during CLACE2.

Similar analysis has also been performed to investigate the effect of local wind speed on the size distributions and mass concentrations of the aerosol chemical components. Over the duration of CLACE2, the local wind speeds varied between 0 and 20 m s^{-1} with an average value of 9 m s^{-1}. Figure 7.13 presents the mass size distributions of the nitrate, sulphate, ammonium and organic components of the aerosol averaged over 'low' and 'high' local wind speed conditions. The 'low' wind speed has been defined as periods where the local wind speed values were below 5 m s^{-1}, while 'high' wind speed corresponds to periods of local wind speed values higher than 10 m s^{-1}. Results show that local wind speed has little influence on the modal behaviour and shape of the mass size distributions of the aerosol chemical components as well as on the organic and sulphate mass concentrations. However, the mass concentrations of nitrate and ammonium appear to increase during periods of 'high' wind speed. This may indicate that particles transported to the Jungfraujoch site at high wind speed conditions are richer in nitrate and ammonium compared to those measured during periods of 'low' wind speed.

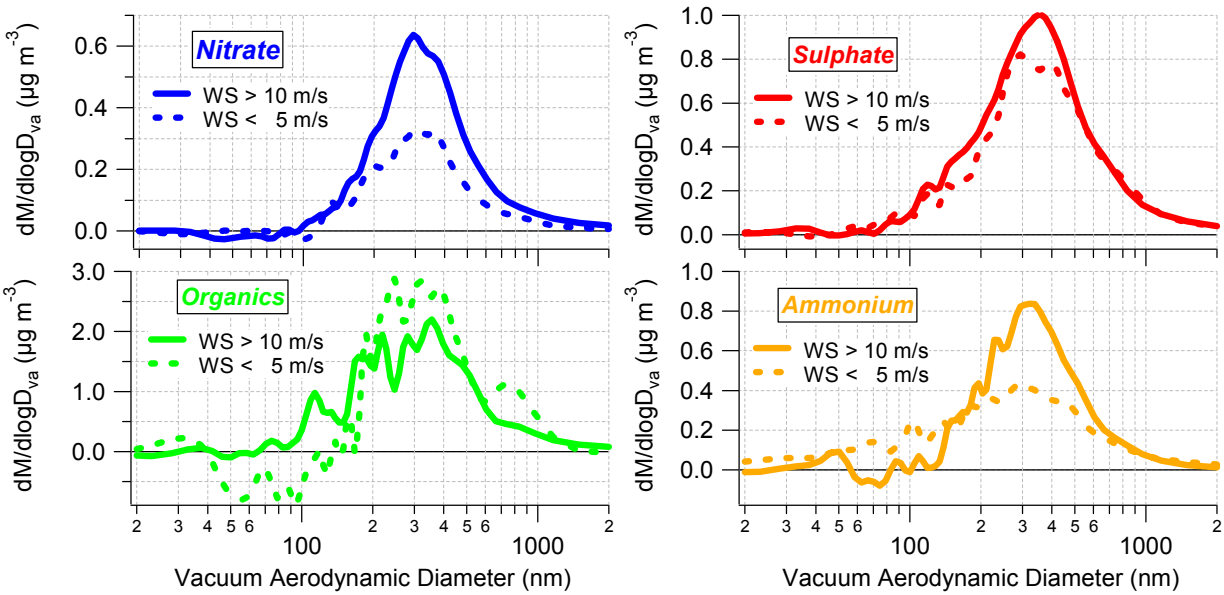

Figure 7.13: Averaged mass size distribution of the aerosol components sampled through the total inlet and separated according to local wind speed during CLACE2.

7.3.4 Classification of aerosol chemical composition and size distribution as a function of air mass history

Air mass back-trajectory analysis has been performed in order to characterise the potential source origins of air masses that reached the Jungfraujoch during CLACE2. Three-day back-trajectories reaching the site at different heights (500 m, 1000 m, and 1500 m above site level; itself at 3580 m asl) were calculated for every 6 hour period during the entire sampling period using the transport and dispersion HYSPLIT4 (Hybrid Single Particle Lagrangian Integrated Trajectories) model available at the US National Oceanic and Atmospheric Administration (NOAA) website (http://www.arl.noaa.gov).

Air masses were classified into five types (A to E) according to their behaviour during the 24 hours prior to sampling. Examples of each type along with the percentage of time each type of air mass was observed throughout CLACE2 are shown in Figure 7.14. Type A refers to air masses that approached the Jungfraujoch from the North West in the previous 24 hours, having often passed over the North Atlantic region and the UK in the previous three days. Air masses in type B approached the site from the West and mostly were over America, the Atlantic Ocean and France in the previous three days. Type B represented the most common type of air masses observed at the Jungfraujoch

during CLACE2, accounting for about 42% of experiment duration. Trajectories reaching the JFJ from the South West after passing over the Iberian Peninsula three days earlier are classified as type C. Air masses of types A - C mostly descended toward the site or were advected at level altitudes. Type D ascended to the site from the South East, after passing over Italy in the previous 24 hours. This type of air masses was only observed during 13% of the time towards the end of the experiment. The last type of air mass, type E, was only observed during the final 24 hours of sampling of the experiment (5% of the time) and approached the site from the NE after passing over central Europe and Southern Germany in the previous 24 hours.

The mass size distributions of the sulphate, nitrate, ammonium and organic fractions of the aerosol averaged according to the above classification of air mass history are summarised in Figure 7.15. The inorganic components of the aerosol appear to have similar mass size distribution shapes with peaks between 200 – 300 nm in all types of air masses. The only exception is for the mass size distribution of nitrate associated with type E air mass, where it appeared to be shifted to a smaller size compared to the sulphate. This may indicate that the aerosol was externally mixed during this period of sampling. However, this type of air mass was only observed during only 5% of the time (the final 24 hours of sampling) and therefore, this behaviour is not reflected in the averaged mass size distribution presented in section 7.3.1. The mass size distribution of the organic fraction of the particles appears to show more variability in the different types of air masses compared to the inorganic distributions. The mass spectral signatures of the organic fractions of the particles associated with each air mass type are presented in Figure 7.16. Each spectrum is averaged over the corresponding periods of each air mass type and the individual mass fragments have been normalised to the total organic mass concentration in that period, providing a quantitative measure of the contribution of the individual mass fragments to the total organic mass for each air mass type.

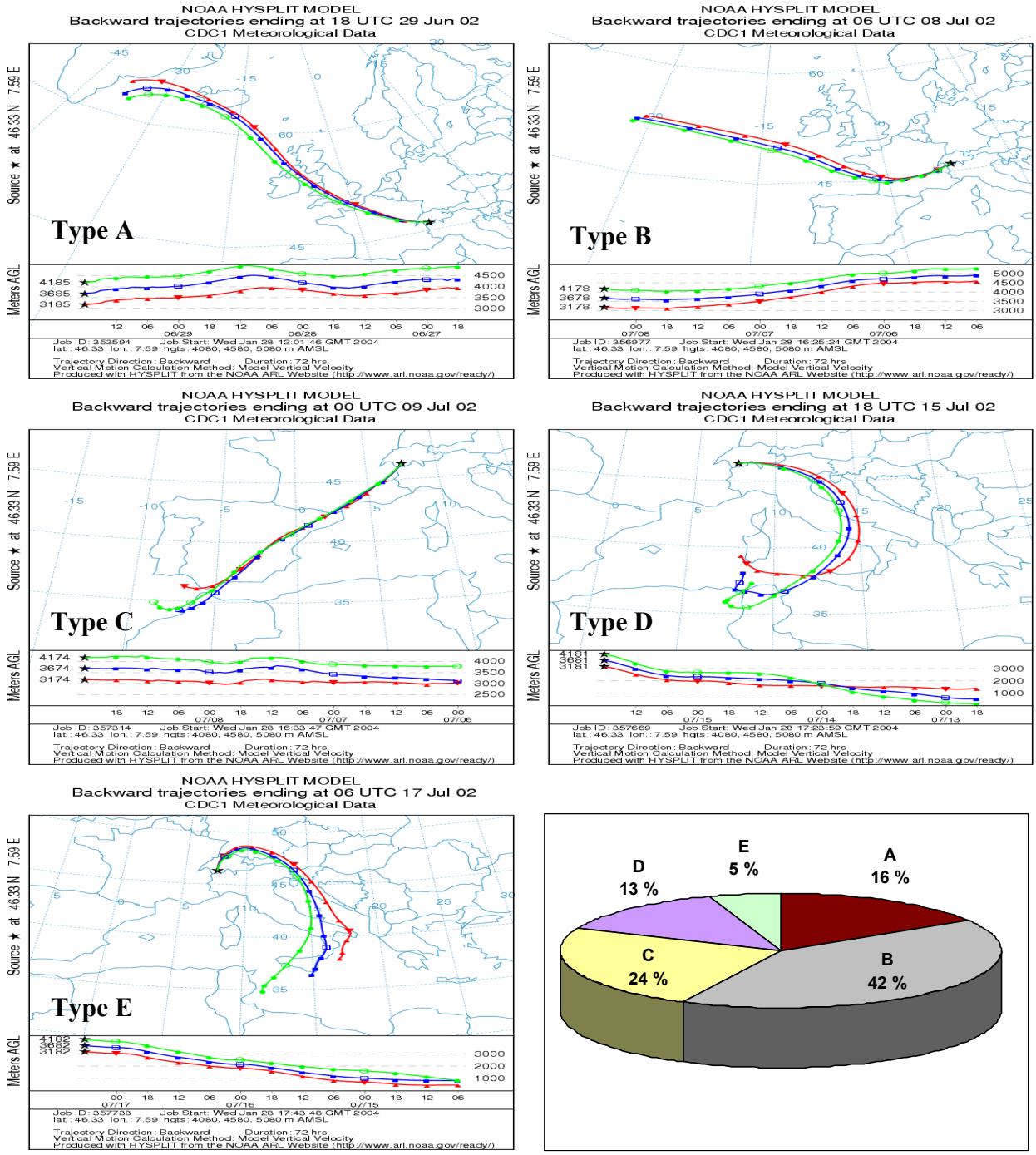

Figure 7.14: Types of air mass observed and the percentage of time each type was sampled during CLACE2. The air masses were classified by 3 day back trajectories calculated the NOAA HYSPLIT model.

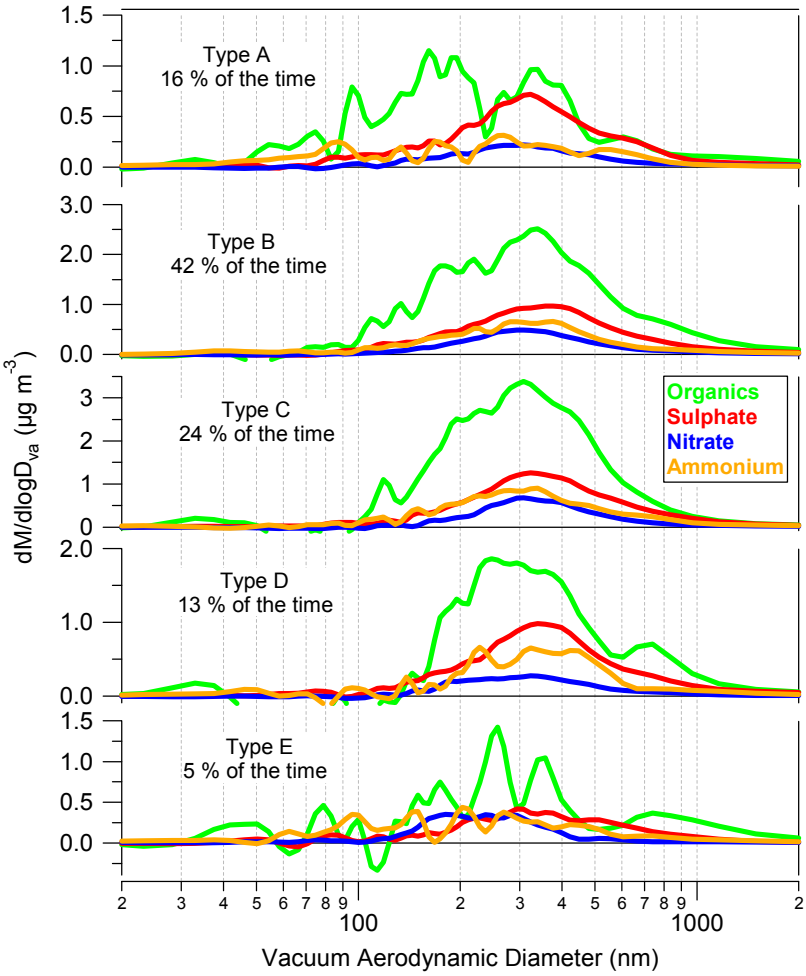

Figure 7.15: Mass size distributions of the aerosol sulphate, nitrate, ammonium and organic components averaged according to the observed types of air masses as classified in Figure 7.14.

The organic mass size distribution associated with type A air masses exhibit a bimodal distribution with one peak below 200 nm and a second peak around 300 – 400 nm, implying that this type of air mass appears to be influenced by anthropogenic pollution. This is consistent with the relatively enhanced contributions of mass fragments 55, 57, 69 and 71 in the organic mass spectral signature associated with this type of air masses as illustrated in Figure 7.16. Type A also shows enhanced 43:44 ratio, also, indicative of more recently polluted air. Anthropogenic pollution appears to have also influenced air masses of type E. In fact the mass spectral signature of the organic fraction of particles in this air mass type shows the lowest contribution of *m/z* 44 to total organic mass (~ 8% compared to an average contribution of 14% in all conditions). On the other hand,

the total organic mass received the highest contribution from *m/z* 43 (9% compared to 7% in all other types of air masses) when the site was influenced by particles associated with this type of air mass. As discussed in Chapter 5, this may indicate higher contribution of hydrocarbons and/or carbonyl-containing compounds. The mass size distributions and mass spectral signatures of the organic particles associated with air masses B, C and D are consistent with highly aged particles with *m/z* 44 contributing about 15% of the total organic mass and negligible contribution of *m/z* 57, the primary organic marker.

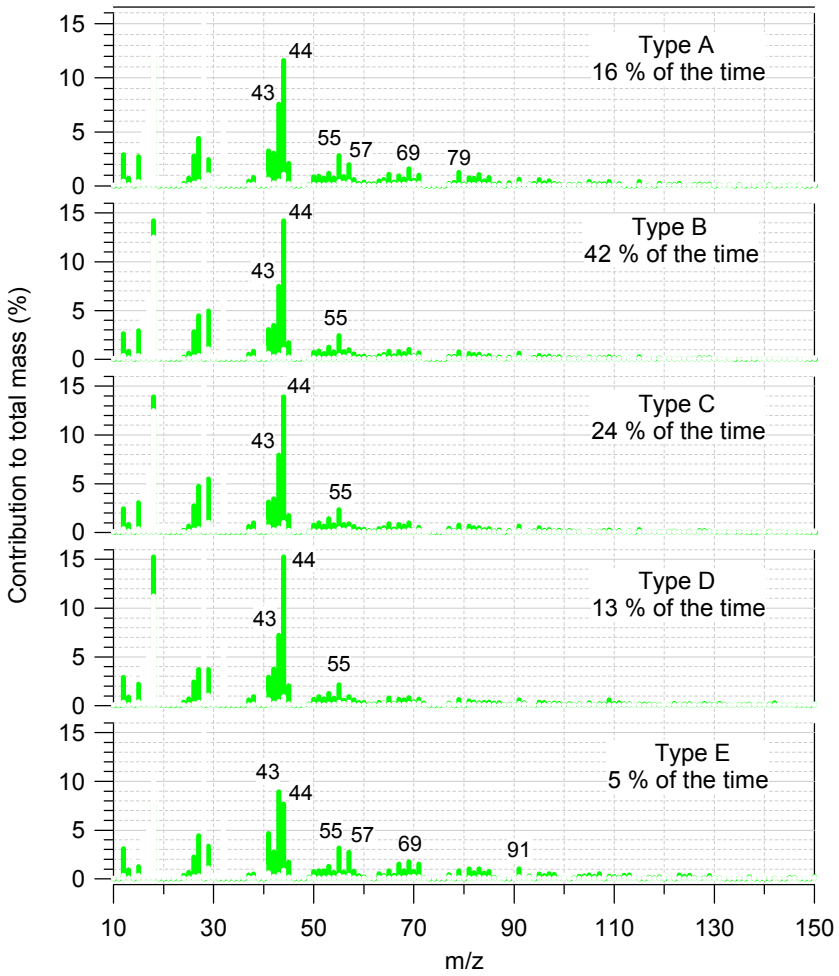

Figure 7.16: Mass spectral signatures of the organic fraction of the aerosol particles averaged according to the observed types of air masses as classified in Figure 7.14.

7.3.5 Hygroscopic properties and chemical composition of aerosols

The hygroscopic properties of aerosol particles sampled through the interstitial inlet were measured using a Hygroscopicity Tandem Differential Mobility Analyser (HTDMA) [*Weingartner et al., 2002*]. A dry monodisperse aerosol of a desired particle diameter (D_0) is selected by a DMA and passed into a humidifier at a well-defined higher RH before it is fed into a chamber with a defined residence time. The aerosol particle diameter (D) at this new RH is then measured using a second DMA and a CPC. The hygroscopic growth factor (GF) of particles is defined as the ratio of the humidified particles diameter to the dry particle diameter (D/D_0) at a defined RH. During CLACE2, the hygroscopic growth factors of three selected particle dry mobility sizes of 50, 100 and 250 nm were performed at 85% RH.

Figure 7.17 show hourly averaged time series of the GF of the three selected dry particle mobility sizes in addition to the inorganic fraction of the total aerosol as measured by the AMS through the interstitial inlet between 08/07 and 16/07/2002. The inorganic fraction was calculated by dividing the sum total of the mass concentration of the sulphate, nitrate and ammonium by the total aerosol mass. Results show that the hygroscopic growth factor values decrease with decreasing particle size. This is consistent with the conclusion made earlier about the increasing dominance of organic particles with decreasing particle sizes at the Jungfraujoch (see section 7.3.1 and Figure

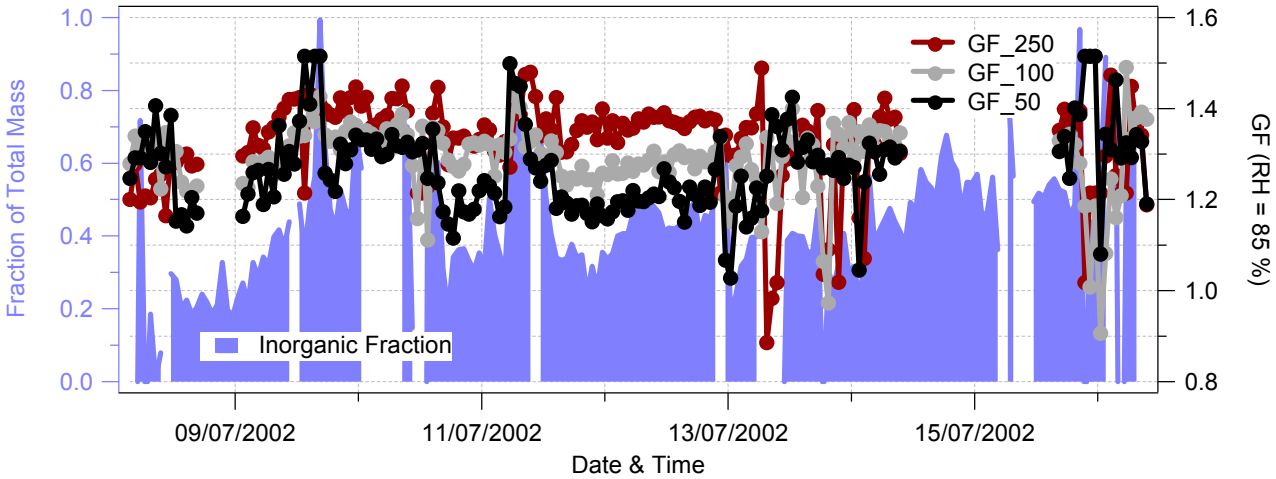

Figure 7.17: Hourly averaged aerosol inorganic mass fraction and growth factor (GF) values of aerosol particles of 50, 100 and 150 nm dry sizes sampled through the interstitial inlet.

7.7). In addition, the GF data show only one hygroscopic mode at any time. This is different to HTDMA measurements made at locations closer to particle sources, where two distinct modes were typically observed and have been termed "more" and "less" hygroscopic [*Cubison et al., 2003; Cubison et al., 2004*]. The observed single hygroscopic mode at the Jungfraujoch implies that particles were internally mixed during the sampling period identified above. For particles with 250 nm dry mobility sizes, the observed GF values were mostly between 1.2 and 1.5 and appeared to increase during periods where substantial increase in the inorganic fraction was observed.

The variability of the GF values of particles with 250 nm dry mobility size as a function of the aerosol chemical composition is illustrated in Figure 7.18. The figure presents a scatter plot of the measured GF values with the ratio of the aerosol inorganic to organic components as measured for all particles sampled through the interstitial inlet. Results indicate that lower GF values were associated with increasing organic mass fraction (mainly inorganic/organic ratios below 0.5). Conversely, increasing inorganic mass fraction result in higher GF values. These results illustrate that when the organic components dominate the aerosol composition, they control its water content. However, when inorganic fraction are more dominant, the particle water content is almost independent of the organic fraction. If an organic surface film is present then its effect on the growth factor would be limited.

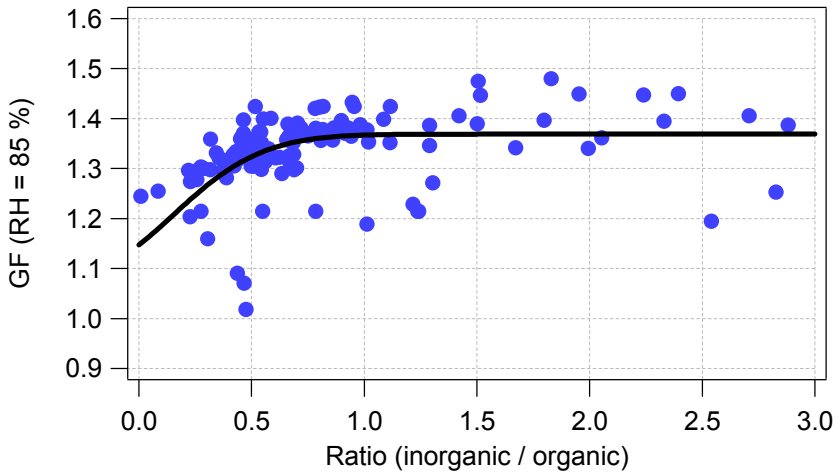

Figure 7.18: Effect of the chemical composition on the hygroscopic growth factor of particles with 250 nm dry size, measured at 85% RH. The solid line is an empirical data fit for visual guidance.

7.4 Cloud Aerosol Interaction

7.4.1 Relationship between Cloud and Aerosol Number Concentrations

The first two panels of Figure 7.19 show a scatter plot of the cloud droplet number concentration (measured by the FSSP) versus the total aerosol number concentration (measured by the CPC using the total inlet) for the entire sampling period with the switching inlet system. Data points are coloured as a function of local wind direction and speed in the top and middle panels, respectively. As discussed in section 7.3.1, relatively high aerosol number and mass concentrations were observed during periods of thermal convection carrying pollution up to the Jungfraujoch site from the growing planetary boundary layer, while lower particle concentrations were indicative of clean, background conditions. It has also been discussed in section 7.3.3.2, that the location of the Jungfraujoch between two mountains channels the local horizontal wind flow in a NW or SE direction. With NW wind direction, air from the Swiss plateau is advected to the Jungfraujoch, while during SE direction the air comes from the inner Alpine area.

The data in the top panel of Figure 7.19 illustrate that relatively high levels of pollution were associated with local wind direction from the SE (particle number concentrations up to 4000 cm^{-3}), whereas the NW direction was associated with cleaner conditions with particle number concentrations mostly below 1000 cm^{-3}. These results are consistent with the findings in section 7.3.3.2, which illustrated that the mass concentrations of the aerosol chemical components observed during SE wind direction were higher than those observed during NW conditions. Data in Figure 7.19 show that droplet number concentrations were also much higher during this period and most likely show the influence of increased aerosol number controlling cloud droplet number. During more polluted conditions that were only experienced in SE conditions the correlation between cloud droplet number and aerosol number appeared to be much lower compared to the clean conditions, but seemed to increase with increasing wind speed, suggesting that high updraft velocities increase particle activation during polluted periods.

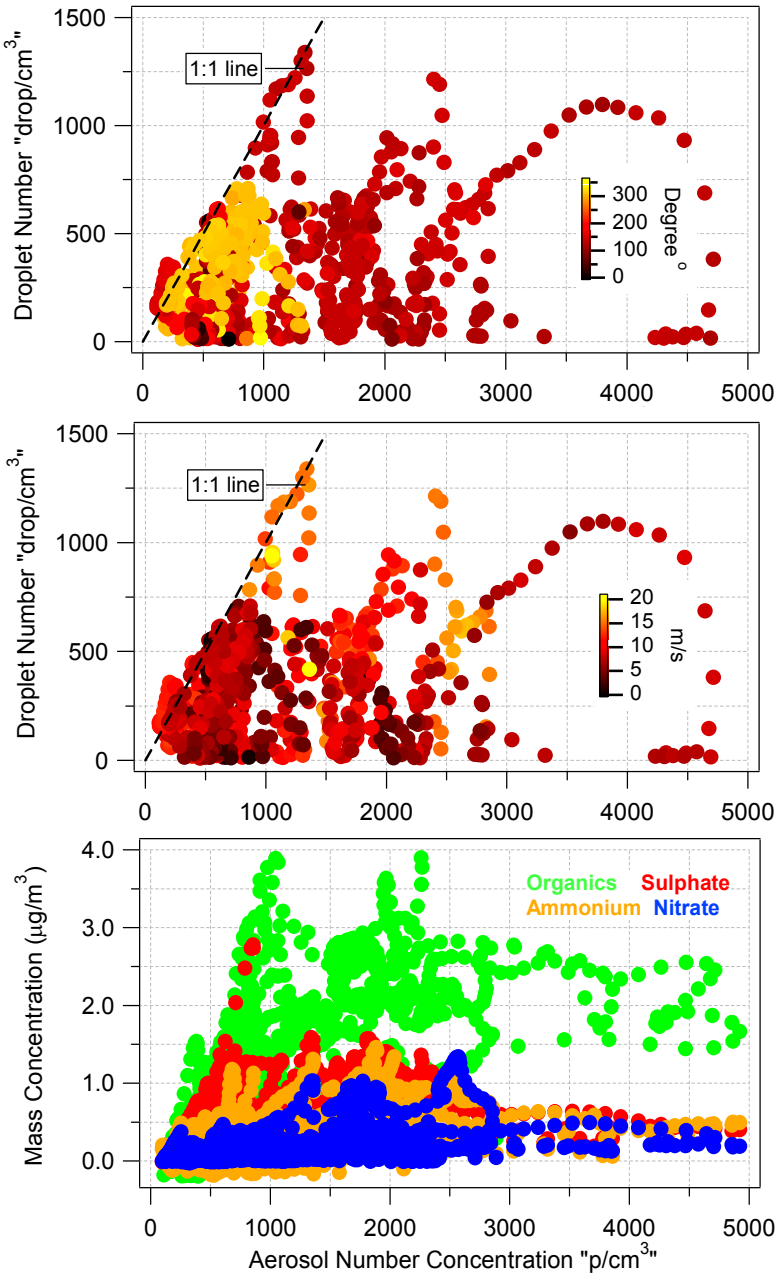

Figure 7.19: The top and middle panels show scatter plots of the cloud droplet number concentration versus aerosol number concentration coloured according to wind direction and wind speed, respectively. The bottom panel shows a scatter plot of the mass concentration of the aerosol chemical components versus the aerosol number concentration.

The near to one-to-one correlation between cloud droplet number and aerosol number observed at low concentrations and the reduction in the ratio at high particle number concentrations during pollution events are consistent with previous measurements of

pre-cloud aerosols and cloud droplets in Manchester, UK and Tenerife, Spain [*Bower et al., 2000a; Bower et al., 2000b*]. The bottom panel in Figure 7.19 presents a scatter plot of the mass concentrations of the major aerosol chemical components measured by the AMS through the total inlet versus the total aerosol number concentration measured by the CPC through the same inlet. It shows that the organic fraction of aerosol dominates the aerosol chemical composition during polluted periods, while comparable concentrations of the different chemical components were observed during most of the clean conditions. The relationship between cloud droplets and the aerosol chemical composition is discussed in more detail next.

7.4.2 Scavenging of Aerosol Chemical Components by Cloud Droplets

To quantify the incorporation of aerosol particles into cloud droplets, a mass scavenging ratio, *F*, has been defined as follows [*Junge, 1963; Hobbs, 1993*]

$$F = \frac{aerosol_{Cloud}}{aerosol_{Total}} = \frac{aerosol_{Total} - aerosol_{Interstitial}}{aerosol_{Total}} \tag{7.1}$$

where $aerosol_{Total}$ is the total aerosol mass concentration (i.e. the sum of particles that were activated or scavenged plus those that remained interstitial. Activated aerosol are particles that have passed their critical supersaturation, however it may be that some aerosol, whilst still unactivated are sufficiently large from taking on water at high humidity that they are sampled as cloud droplets. Conversely, some activated cloud droplets, especially close to cloud base, may not have grown sufficiently to be sampled as cloud droplets. The interstitial inlet therefore provides an operational size cut (1 μm) set approximately larger than most ambient aerosol and below that of most cloud droplets. Particles sampled through the latter inlet are referred to as $aerosol_{Interstitial}$. The difference between $aerosol_{Total}$ and $aerosol_{Interstitial}$ is defined as $aerosol_{Cloud}$ and represents the aerosol in the cloud droplets. The mass scavenging ratio defined above is also known as the activated fraction and it may vary from zero to unity. The same definition has also been applied on the basis of number concentration instead of mass concentration [*Gillani et al., 1995*].

Equation 7.1 has been used to calculate the mass scavenging ratios of the sulphate, F_{SO4}, Nitrate, F_{NO3}, Ammonium, F_{NH4}, and Organic, F_{Org}, fractions of the ambient aerosol at the Jungfraujoch as measured by the AMS, providing probably the first on-line, highly time resolved measurements of these ratios. The bottom half of each panel in Figure 7.20 presents hourly averaged time series of the mass concentrations of the nitrate, sulphate, ammonium and organic fractions of the aerosol sampled through the total and interstitial inlets. The top half of each panel represents an hourly averaged mass scavenging ratio for the corresponding chemical component calculated by equation 7.1. The blue and gray background colours are indication of clear and cloudy conditions, determined using a cloud droplet number concentration threshold of 10 cm^{-3}. The gaps in the classification are due to a lack of FSSP data during those periods. It is important to note that low signal to noise levels during periods when mass concentrations are close to zero may result in unreasonably high or low scavenging ratios for brief periods of time, such as the high F_{NO3} value on the 11th July.

Results show that all four chemical components, including organics, appear to be scavenged by cloud droplets. Within the same in-cloud event, the scavenging ratios of the different components were found to be of similar values. However, variable mass scavenging ratios ranging between 0.3 and ~ 1 were observed for the same chemical species in different cloud events. The characteristics of individual cloud events and their influence on the mass scavenging ratios of the aerosol chemical components and size distributions are discussed in section 7.4.4. In order to compare the mass scavenging ratios of the different chemical components of the aerosol, the ratios of F_{NO3}, F_{NH4} and F_{Org} to F_{SO4} were calculated and plotted against the ratio of cloud droplet number concentration to aerosol number concentration in Figure 7.21. The latter ratio is a measure of the scavenging of aerosol particles by cloud droplets, where a ratio of unity means that all available aerosol particles are incorporated into cloud droplets, while a ratio close to zero indicates that aerosol particles are mainly present in the interstitial population. The mass scavenging ratio of sulphate has been chosen as the base ratio for comparison with the scavenging ratios of other chemical components because sulphate is commonly measured in cloud droplets, and the scavenging and subsequent oxidation of gas phase SO_2 by cloud droplets have been reported to be of minor importance at the

Jungfraujoch due to the usually low SO_2 concentrations at this site [*Baltensperger et al., 1998*].

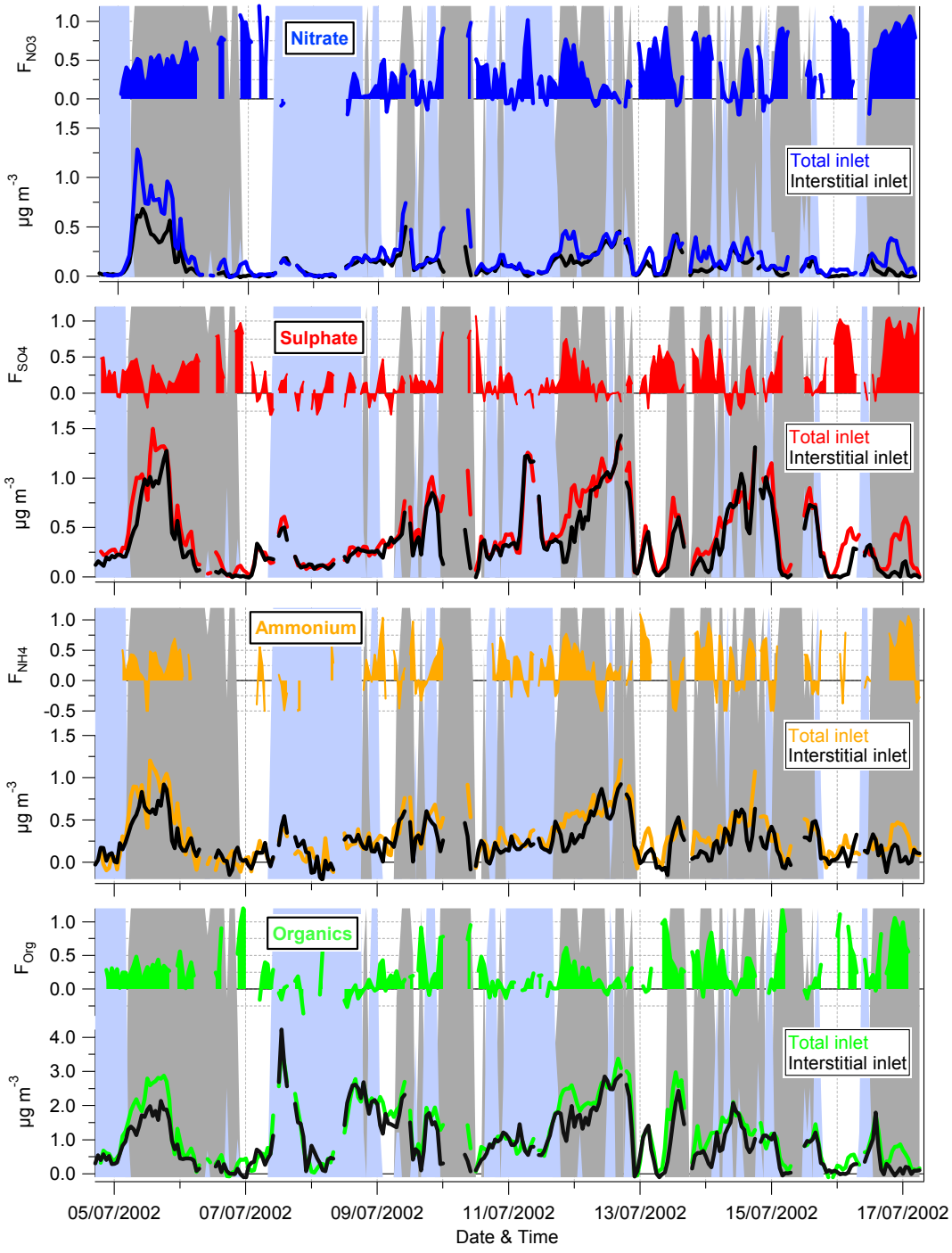

Figure 7.20: The bottom half of each panel shows the hourly averaged mass concentrations of the corresponding species sampled through the total and interstitial inlets, while the top half presents the mass scavenging ratio calculated using equation 7.1. The blue and gray colours in the background are indication of clear and cloudy periods.

Results in Figure 7.21 show that the ratios of F_{NO3}/F_{SO4}, F_{NH4}/F_{SO4} and F_{Org}/F_{SO4} vary little with the increase of aerosol particle scavenging by cloud droplets, suggesting that the aerosol chemical components are internally mixed. This result is consistent with the single hygroscopic growth mode observed in the HTDMA data presented in section 7.3.5. The noticeable variability in the ratios of mass scavenging ratio at low number scavenging ratio arise because the data in Figure 7.21 are mostly within the propagated errors (error bars are not shown for clarity).

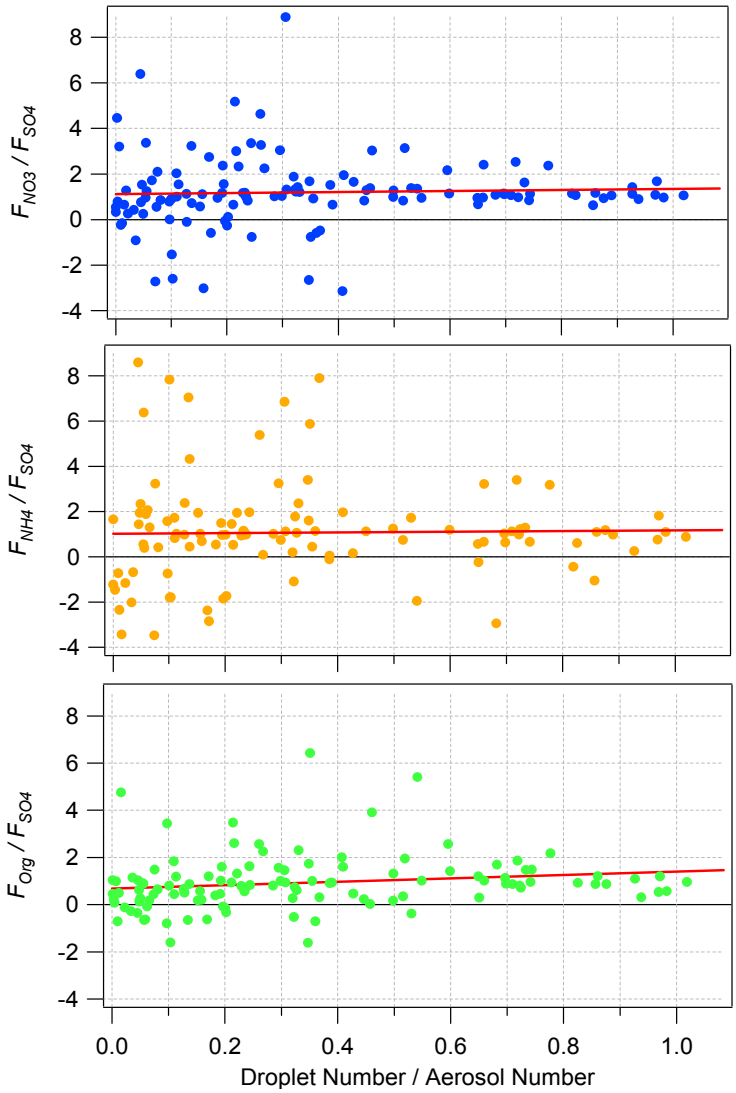

Figure 7.21: Comparison of the mass scavenging ratios of nitrate, ammonium and organics to that of sulphate as a function of cloud droplet number to aerosol number ratio (see text for details).

Mass size distributions of the nitrate, sulphate, ammonium and organic fractions of the aerosol were measured through the total and interstitial inlets and averaged over all cloudy periods throughout the entire duration of the experiment where the switching inlet was in use. The data are shown in Figure 7.22. The differences between the total and interstitial inlet distributions are also shown for each species. Although these averages include different cloud events, which are likely to have different chemical as well as microphysical properties, the distributions and their differences provide an overall indication of the mass size distributions for all species and their scavenged fraction as a function of particle size. The differences in the mass size distributions from the two inlets indicate that the scavenged particles are mostly larger than approximately 150 nm, though there is some evidence that nitrate is activated down to 100 nm. Detailed analyses of the aerosol chemical composition and size distributions as well as cloud microphysical properties during selected individual cloud events are presented and discussed in section 7.4.3.

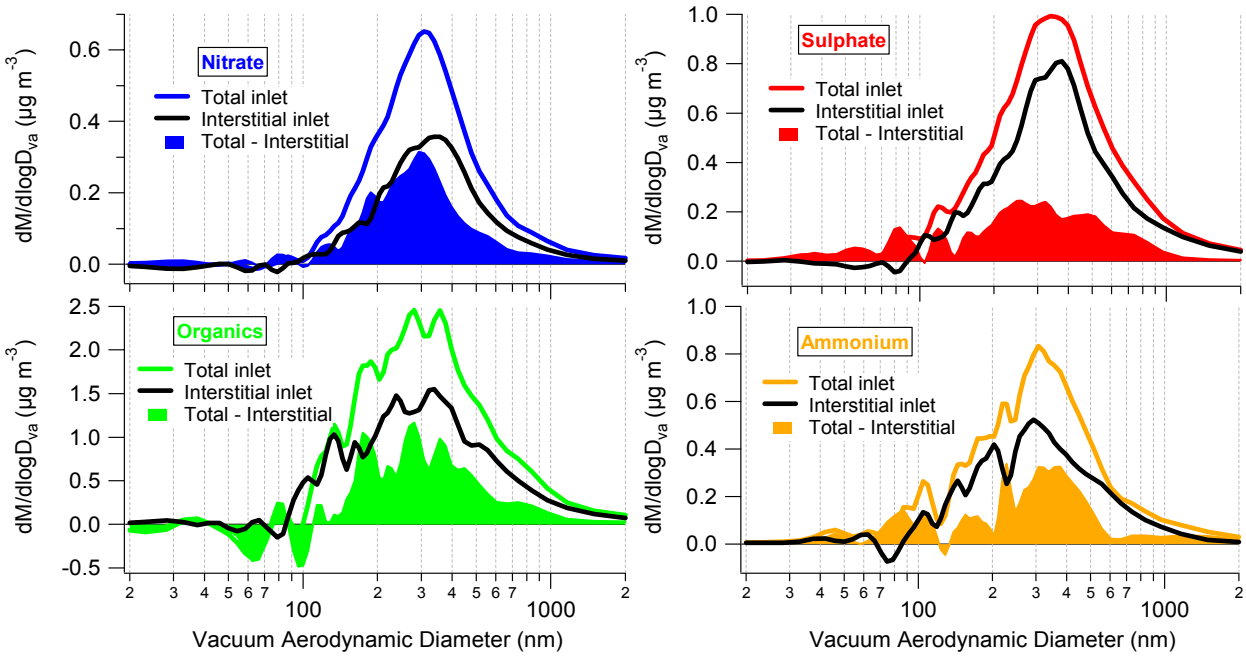

Figure 7.22: Mass size distributions of the aerosol chemical components measured through the total and interstitial inlets averaged over all cloudy periods during CLACE2. The difference between the total and interstitial distributions for is also shown for each species.

7.4.3 Cloud-Aerosol Interaction: Case Studies

Detailed analyses of a number of cloud events have been performed in order to investigate the effect of aerosol particles on the cloud properties and to characterise the chemical composition and size distribution of the activated aerosol particles. Case studies have been selected on the basis of the consistency of the cloud droplet number concentration and size distribution as measured by the FSSP. A total of six case studies have been identified and their corresponding durations are listed in Table 7.2.

Case study 1	05:31 05/07/2002 – 16:31 05/07/2002
Case study 2	22:10 05/07/2002 – 05:15 06/07/2002
Case study 3	19:46 11/07/2002 – 22:44 11/07/2002
Case study 4	00:00 14/07/2002 – 03:00 14/07/2002
Case study 5	14:38 14/07/2002 – 18:23 14/07/2002
Case study 6	19:43 16/07/2002 – 00:30 17/07/2002

Table 7.2: A list of the times and dates of the selected cloud-aerosol interaction case studies

Table 7.3 presents a summary of the cloud and aerosol measurements and meteorological conditions during each of the case studies. All reported values are averages over the duration of the corresponding case study as listed in Table 7.2. The reported aerosol number and mass concentrations of the chemical components are those measured using the total inlet. The liquid water content per droplet (LWC) has been calculated by dividing the measured cloud liquid water content by the cloud droplet number concentration. F_{number} is the aerosol number scavenging ratio, which is defined in a similar way as the mass scavenging ratio described in equation 7.1 (section 7.4.2), except it is calculated using the total and interstitial aerosol number concentrations measured by the CPC.

	Case study 1	Case study 2	Case study 3	Case study 4	Case study 5	Case study 6
Cloud properties						
Cloud number conc.	598	581	906	483	485	492
LWC (mg drop^{-1})	0.45	1.02	0.66	0.84	2.35	1.42
Droplet mode diameter (µm)	8	8 – 15	11	12	11 & 25	10 – 20
Aerosol number-based properties						
Aerosol number conc. (cm^{-3})	2159	1518	3573	537	636	728
F_{number}	0.15	0.13	0.16	0.28	0.19	0.34
Aerosol mass-based properties						
Total SO4 (µg m^{-3})	1.04	0.46	0.57	0.26	0.83	0.41
F_{SO4}	0.35	0.34	0.67	0.74	0.27	0.90
Total NO3 (µg m^{-3})	0.89	0.26	0.42	0.25	0.31	0.34
F_{NO3}	0.43	0.56	0.66	0.79	0.51	0.87
Total NH4 (µg m^{-3})	0.88	0.36	0.50	0.23	0.61	0.45
F_{NH4}	0.35	0.46	0.70	0.83	0.61	0.72
Total Org (µg m^{-3})	2.30	0.77	2.48	1.02	1.28	0.76
F_{Org}	0.31	0.38	0.50	0.75	0.41	0.92
Organic / total mass	0.46	0.42	0.62	0.58	0.42	0.39
M/z 44 /total organic	0.13	0.08	0.12	0.13	0.18	0.14
Meteorological Conditions						
Wind speed (m s^{-1})	13.8	9.72	7.34	3.78	7.61	8.48
Wind direction	SE	SE	SE	SE	SE	NW
Air mass type	B	B	B	B	D	E

Table 7.3: Summary of cloud properties, aerosol number- and mass-based properties measured through the total inlet and meteorological conditions averaged over the durations of the selected case studies as listed in Table 6.2.

The cloud events in the six case studies can be classified into two types based on the observed aerosol number concentration. The first type includes cases 1 to 3 and represents periods of high aerosol number concentration (> 1500 cm^{-3}), i.e. 'polluted' cases. The second type includes the other three cases and is associated with lower aerosol number concentrations (< 800 cm^{-3}), i.e. 'clean' cases. The data show that higher cloud droplet number concentrations and small droplet sizes were associated with higher aerosol number concentrations at the Jungfraujoch during CLACE2. These findings are consistent with the Twomey hypothesis that increased aerosol number concentrations result in higher cloud droplet concentrations and reduced droplet sizes [*Twomey, 1977*]. This effect increases the cloud's optical depth, its scattering of sunlight back to space and hence increases its cooling effect and is otherwise known as the first indirect effect radiative forcing effect of aerosols on climate [*Charlson and*

Heintzenberg, 1995]. This observation is similar to previous results obtained at the Jungfraujoch [*Baltensperger et al., 1998*], and provides additional evidence for a possible impact of anthropogenic aerosols on cloud albedo.

Low number scavenging ratios are expected in clouds influenced by anthropogenic sources because of the prevalence of fine aerosol particles; number scavenging ratios less then 0.1 are expected in most such situations. Seinfeld and Pandis (1998) stated that only in clouds in the remote marine atmosphere does the total number scavenging ratio exceed 0.1. The value of the total number scavenging ratio, F_{number}, during the periods of the six case studies varied between 0.13 and 0.34 and appeared to be higher during the 'clean' case studies relative to the 'polluted' ones. These results suggest that this ratio can exceed 0.1 not only in remote marine atmospheres but also at remote, high-alpine locations.

Inspection of the mass scavenging ratios of the individual aerosol chemical components in Table 7.3 reveals that lowest ratios for all components are found in the 'polluted' cases number 1 and 2, while the highest values are associated with the 'clean' cases number 5 and 6. These results are consistent with the total number scavenging ratios and imply that particles associated with anthropogenic pollution have lower scavenging ratios compared to aged particles. In fact, mass scavenging ratios close to unity were observed in case study number 6, which is the only case study that is associated with the 'cleaner' NW wind direction (see section 7.3.32). However, relatively high mass scavenging ratios were observed during the 'polluted' case study number 3, and relatively low mass scavenging ratios were observed during the 'clean' case study number 5. At first glance this may appear inconsistent but it may be related to the ageing of polluted aerosol. The AMS data are used to investigate the link between scavenging ratio and composition in the following section.

Averaged mass size distributions of the aerosol chemical components (sampled through the total inlet) during each of the case studies are shown in Figure 7.23. Results reveal that the aerosol organic fraction exhibits broad distributions with substantial mass associated with particle sizes below 200 nm during the 'polluted' case studies (cases 1 –

3). The calculated organic mass scavenging ratio, F_{Org}, reached its lowest values of 0.31 and 0.38 during case numbers 1 and 2, respectively, where significant fraction of the organic mass was associated with small particles. The value of F_{Org} increased to 0.50 during case study 3, where 'larger' organic particles increased substantially, compared to the first two cases.

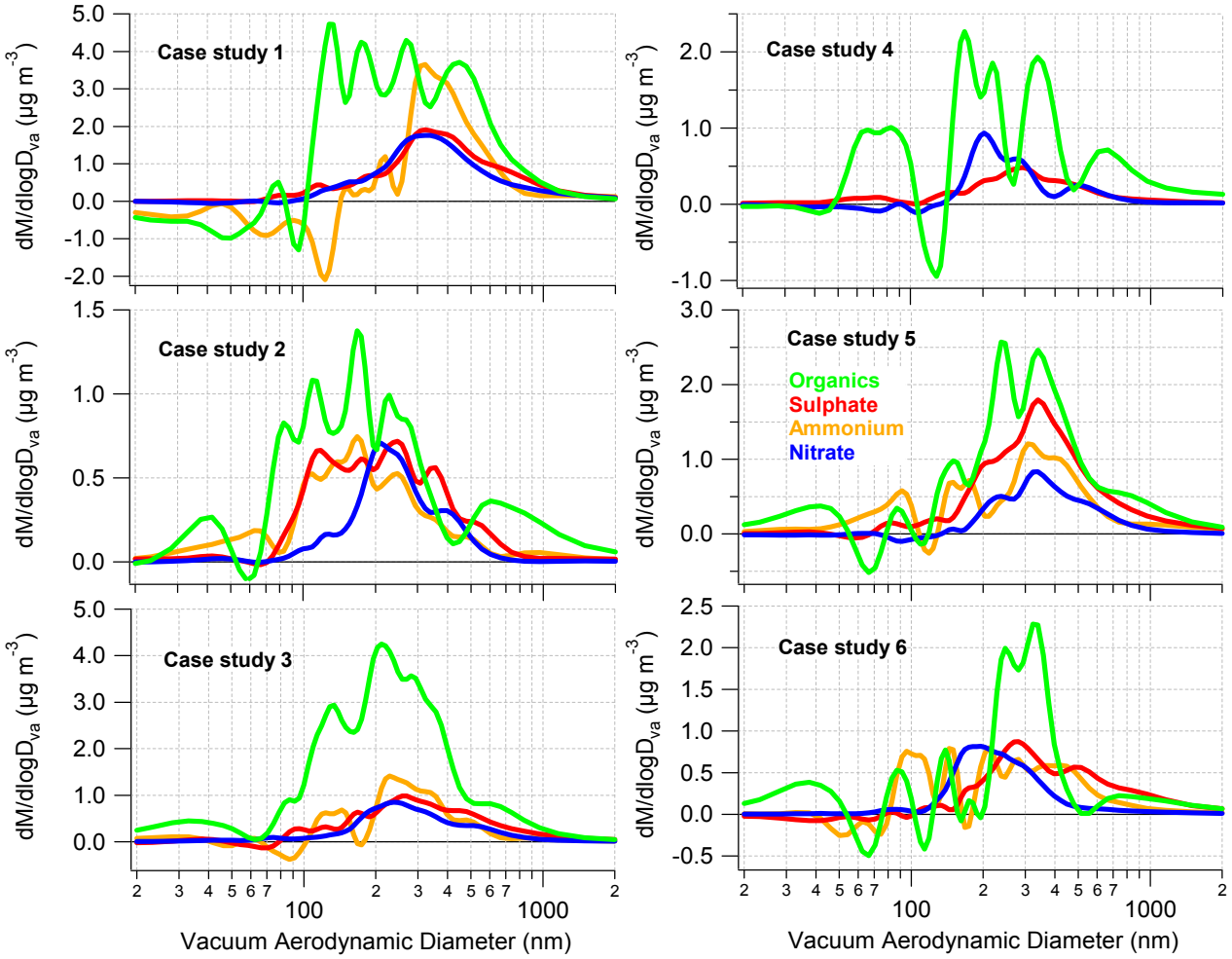

Figure 7.23: Mass size distributions of the aerosol chemical components, sampled through the total inlet and averaged over the durations of the corresponding case studies as listed in Table 7.2. The ammonium distribution is not shown for case study number 4 due to the low signal to noise associated with the ammonium mass fragments during the corresponding period.

The mass spectral signatures of the aerosol organic fraction during the individual case studies are shown in Figure 7.24. The individual organic mass fragments in each spectrum have been normalised to the total organic mass, providing a quantitative measure of their percentage contribution to the organic total mass. The organic

signature in the first and third case studies is consistent with aged aerosol, where *m/z* 44 was the dominant mass fragment and accounted for 13 and 12%, respectively, of the total organic mass. On the other hand, a different mass spectral signature was observed during the case study number 2, where *m/z* 44 accounted for only 8% of the total organic mass. Cloud droplets associated with the second case study had the highest liquid water content relative to the other two 'polluted' cases, whereas the aerosol an cloud droplet numbers were similar, implying a lower cloud base in the second case study. These results suggest that the relatively high mass scavenging ratios observed during case study number 3 compared to those in cases number 1 and 2 may be attributed to more aerosol aging in the former case.

The above conclusion is further supported by the observed high mass scavenging ratios and the lack of small particles in the mass size distributions of the aerosol components in case studies number 5 and 6. In case number 4, there is some evidence for organic mass at smaller sizes but the concentrations are low and almost all of the mass is contained in the larger aerosol that may act as CCN. The organic mass spectral signatures associated with case studies 4 and 6 in Figure 7.24 are typical of aged particles, with *m/z* 44 contributing 13 and 14% to the total organic mass, respectively. Although case study number 5 has been classified as 'clean', the observed mass scavenging ratios are considerably lower compared to the other two cases with the same classification. The measured cloud droplets during this case study have a bimodal size distribution as illustrated in Figure 7.25, indicating that two types of cloud droplets were present during this period. The first type of cloud droplets had a modal diameter at about 11 μm, while the second type of droplets were much larger with a modal diameter at about 25 μm. The different droplet modal diameters imply two cloud activation processes. The first activation process is associated with high updraft velocity and results in the small cloud droplets, which typically have low mass scavenging ratios. On the other hand, the second activation process is likely to have occurred at lower updraft velocity and resulted in the activation of larger particles into the observed large cloud droplets. The observed shoulders of small particle sizes in the nitrate and sulphate mass size distributions in Figure 7.23 support the hypothesis.

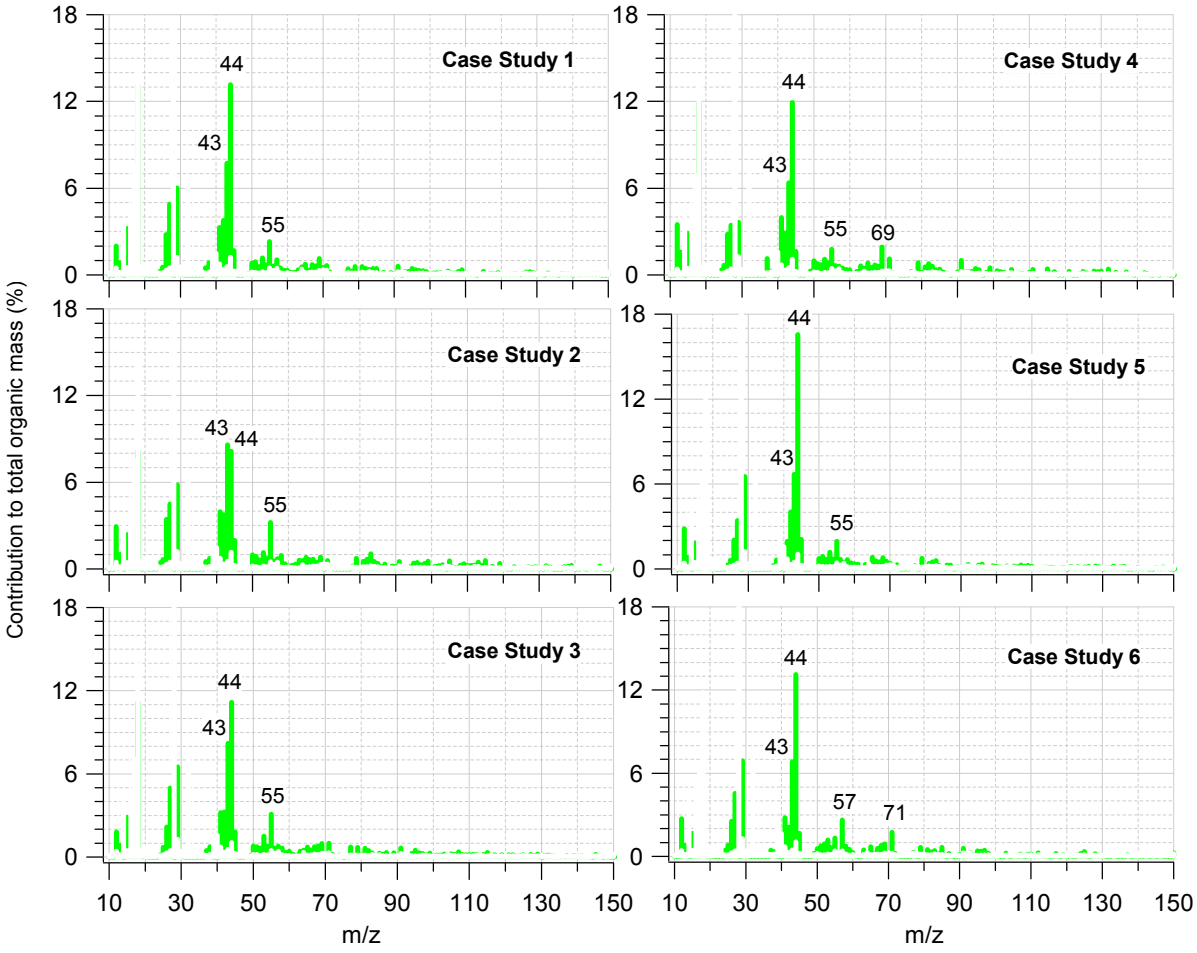

Figure 7.24: Mass spectral signatures of the aerosol organic fraction, sampled through the total inlet and averaged over the durations of the corresponding case studies as listed in Table 7.2. Each spectrum is normalised to the total organic mass in the corresponding period.

These different activation processes are most likely due to the combination of frontal and orographic cloud combining, which was observed at the site on that day. The orographic cloud is most likely rich in ammonium, nitrate and organic, as is common on other days, and because of the strong updraughts in flows up the valley to the site, the aerosol were subjected to high supersaturations during cloud formation. Because of this, many aerosol particles are activated, leading to high cloud droplet numbers and low mean droplet sizes. The frontal cloud, advecting to the site, was most likely formed from regional aerosol, rich in sulphate, as has been observed on other clear sky days (see section 7.3.3.1 and Figure 7.10). These aerosols were not subjected to such

vigorous updrafts and fewer particles were activated, giving fewer, larger cloud droplets.

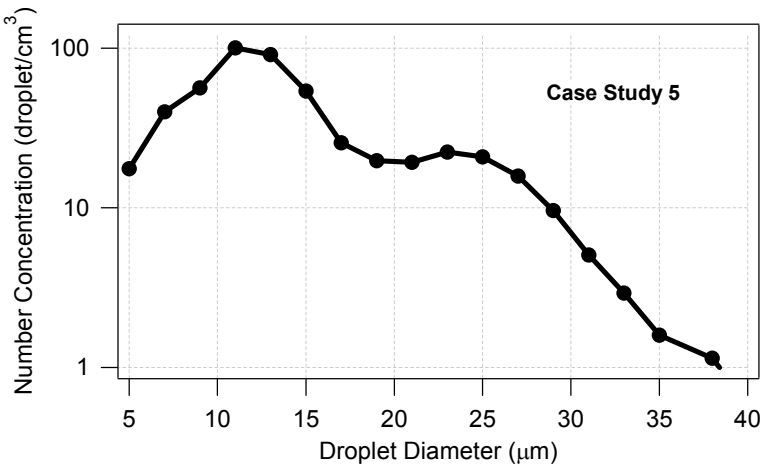

Figure 7.25: Cloud droplet number size distribution measured by the FSSP averaged over the duration of case study number 5 as listed in Table 6.2.

The size-dependent scavenging of the aerosol chemical components can be calculated from the difference in the mass size distributions measured through the total and interstitial inlets. Figure 7.26 illustrates this type of information for the nitrate, sulphate and organic components of the aerosol using case studies number 1 and 6 as examples of 'polluted' and 'clean' conditions, respectively. Nearly complete scavenging of nitrate and sulphate particles larger than 100 nm and organic particles above 200 nm have been observed for the more aged particles in case study number 6. On the other hand, only fractions of the nitrate and organic particles larger than about 150 nm and sulphate particles larger than about 300 nm were scavenged in the more polluted case study number 1. The size-dependent scavenging of the same three components are also shown, in same figure, for case study number 5 because of the unique microphysical properties of its cloud droplets. The observed bimodal size distributions of scavenged fractions of the nitrate, sulphate and organics, in addition to the increasing scavenged fractions as a function of particle size are additional evidence of the hypothesis above that two types of cloud droplet activation occurred during this case study.

The contribution of the organic fraction to aerosol total mass, as well as the contribution of *m/z* 44 to the total organic mass for the six case studies are summarised in Table 7.3.

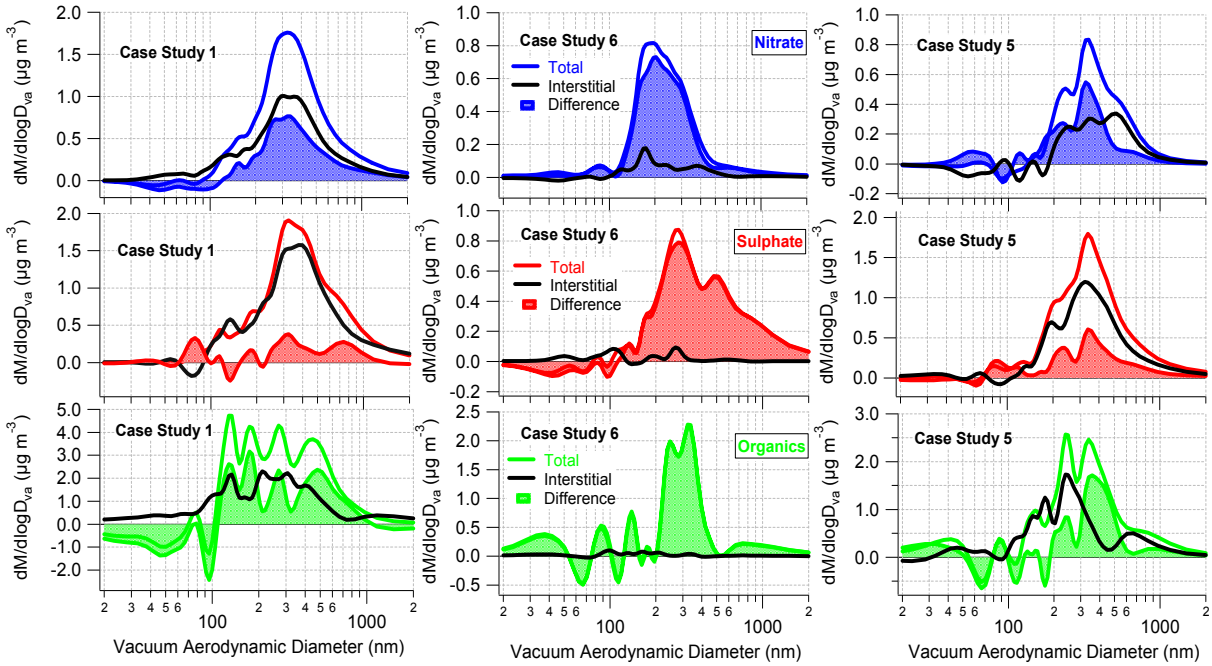

Figure 7.26: Size-dependent mass scavenging of the nitrate, sulphate and organic components of aerosol particles observed in case studies number 1, 6 and 5. The corresponding durations are listed in Table 7.2.

One of the main aims of these case studies is to provide an insight into the role of organics and their level of oxidation in the particle scavenging process by cloud droplets. The organic contribution to total mass varied between 0.39 and 0.62, while the contribution of *m/z* 44 to the total organic mass ranged from 0.08 to 0.18. The highest mass scavenging ratios were observed in case study number 6, where the lowest organic contribution to total mass (0.39) and the second highest contribution of *m/z* 44 to total organic mass (0.14) were observed. On the other hand, the highest mass scavenging ratios during the 'polluted' events were observed in case study number 3, where the highest organic contribution to total mass (0.62) was observed. During this case study, the organic signature and size distribution were representative of aged particles. These results suggest that ageing and processing of atmospheric organic aerosol increases their ability to act as cloud condensation nuclei (CCN).

7.5 Summary

The second Cloud and Aerosol Characterisation Experiment (CLACE2) took place in the summer of 2002 at the Jungfraujoch mountain top research station in the Swiss Alps. The experiment aimed to couple the highly time and size-resolved chemical

composition information from the AMS to a suite of other aerosol and microphysical instruments in a variety of air masses in the lower free troposphere at the Jungfraujoch in order to investigate the interaction between cloud and aerosols. Results showed that organic material accounted, on average, for 54% of the total measured aerosol mass at the Jungfraujoch during CLACE2. All aerosol components showed diurnal patterns with the mean values of their mass concentrations exhibiting a maximum during the afternoon and evening hours, and a minimum during the early hours. A single distinct mode with a peak between 300 - 400 nm was observed for all of the aerosol components. In addition, the organic mass size distribution appears to be broader, compared to the inorganic species, with a shoulder at about 200 nm. Results indicated that the organic fraction of the aerosol at the Jungfraujoch was largely composed of highly oxidised compounds and that secondary organic aerosols were more significant than primary compounds. Compounds such as carbonyls and dicarboxylic- and poly-acids were found to dominate the organic composition. Results showed that *m/z* 44, the AMS signature of oxidised organic compounds and humic-like substances, accounts, on average, for about 14% of the total organic mass at the Jungfraujoch.

Air masses arriving at the sampling site during CLACE2 were classified into five types according to their behaviour during the 24 hours prior to sampling. The mass size distribution of the organic fraction of the particles appears to show more variability in the different types of air masses compared to the inorganic distributions. HTDMA measurements showed that a single hygroscopic mode was mostly observed at the Jungfraujoch, implying that particles were internally mixed during this experiment. For particles with 250 nm dry mobility sizes, the observed GF values were mostly between 1.2 and 1.5 and appeared to increase during periods where substantial increase in the inorganic fraction was observed. Results indicated that lower GF values were associated with increasing organic mass fraction. Conversely, increasing inorganic mass fraction result in higher GF values.

Most of the clouds observed at the Jungfraujoch during CLACE2 were formed by lifting of air masses rather than by regional high-level advection. The modal behaviours and shapes of the mass size distributions of the individual aerosol chemical components did

not appear to vary between in- and out- of cloud conditions. On the other hand, the mass concentrations of the inorganic components were enhanced during cloudy periods, while this did not appear to be the case for the organic fraction of the particles. These results imply that significant fraction of the inorganic mass observed at the Jungfraujoch was associated with cloud events, while the organic mass concentration appeared to be similar during in and out of cloud events.

Near one-to-one correlation between cloud droplet number and aerosol number was observed during clean conditions, while during more polluted conditions the correlation between cloud droplet number and aerosol number appeared to be much lower, but seemed to increase with increasing wind speed, suggesting that high updraft velocities increase particle activation during polluted periods. Results show that all four chemical components, including organics, appear to be scavenged by cloud droplets. Within the same in-cloud event, the scavenging ratios of the different components were found to be similar in values. However, variable mass scavenging ratios ranging between 0.3 and ~ 1 were observed for the same chemical species in different cloud events. The differences in the mass size distributions from both inlets indicate that the scavenged particles are mostly larger than approximately 150 nm, though there is some evidence that nitrate is activated down to 100 nm.

Analysis based on six cloud case studies showed that the cases where the organic content of the particles was relatively low showed most efficient mass scavenging (case study 6), and the more aged the aerosol is, the more likely it is that it will be scavenged. The mixing state of aerosol particles appeared to be more important than the organic content in the polluted cases. A high degree of internal mixing between the organic and inorganic components of the aerosols resulted in efficient mass scavenging of the organics. This was the case when the organic fraction was highly oxidised (case study 3). However, if the particle number is dominated by small particles (< 200 nm) that are composed almost entirely of organic material then mass and number scavenging is reduced as these particles have a tendency to not grow in a high humidity environment.